To the Graduate Council:

I am submitting herewith a thesis written by Lisa Leigh Satterwhite entitled "Receptor-Mediated Endocytosis of Au_{16}-hCG by Porcine Luteal Cells." I have examined the final copy of this thesis for form and content and recommend that it be accepted in partial fulfillment of the requirements for the degree of Master of Science, with a major in Zoology.

John H. Abel, Major Professor

We have read this thesis
and recommend its acceptance:

Accepted for the Council:

The Graduate School

RECEPTOR-MEDIATED ENDOCYTOSIS OF Au_{16}-hCG BY PORCINE LUTEAL CELLS

A Thesis

Presented for the

Master of Science

Degree

The University of Tennessee, Knoxville

Lisa Leigh Satterwhite

March 1984

ACKNOWLEDGMENTS

I am greatly indebted to Dr. John H. Abel, my thesis advisor and friend, who enthusiastically provided a stimulating introduction to science. I am also grateful to the other members of my committee, Drs. R. Bagby and T. Chen, for their helpful discussions and the use of their equipment.

This work could not have been completed without the technical advise from Dick Williams, the Director of the Electron Microscopy Core Facility.

I am grateful to Michael G. Landen, Margaret Corey Kreyling, Kitty Johansen, and Luann Braswell Toney, who provided valuable instructions as well as friendship.

I am also grateful for my friends in the Gilula laboratory for their continual encouragement.

Finally, I would like to express my deepest appreciation to my parents, Mr. and Mrs. D.H. Satterwhite, and to Alex McMillan, IV for the gift of their time, support, and encouragement throughout the course of this work.

ABSTRACT

Although the plasma membrane of porcine luteal cells from a variety of species has been shown to be actively involved in the binding and internalization of human chorionic gonadotropin (hCG), the intracellular movement and fate of the hormone-receptor complex is not well understood. Previously, internalization of labeled hormone and a variety of membrane constituents was thought to occur in luteal cells in vivo via coated pits that transferred their contents to secondary lysosomes. Rarely was tracer observed between the cell surface and lysosomes except in a series of tenuous smooth surfaced canaliculi positioned directly beneath the plasma membrane. In order to more closely examine endocytosis of hormone by luteal cells in vitro a series of labeling experiments were initiated where cells were allowed to internalize a well characterized complex of Au_{16}-hCG. Porcine luteal cells, cultured following collagenase dispersal, were shown to bind ^{125}I-hCG. Binding was both specific, as indicated by the effective cold competition by native hormone, and saturable after 60 min at 37°C. Luteal cells that were incubated with Au_{16}-hCG for 4 min. at 4°C, and processed for electron microscopy, were observed to bind Au_{16}-hCG diffusely to the microvillar extensions along the cell surface. Following warming to 37°C, Au_{16}-hCG was observed to form small clusters along the cell surface, and to be internalized in coated vesicles. Following endocytosis, gold beads were observed in smooth surfaced vesicles termed initial endosomes that were located directly beneath the plasma membrane. Multivesicular bodies (mvb) distributed near the perimeters of the cells also were observed to accumulate gold particles. After 90 min., gold

beads were present in secondary endosomes located deep within the centrospheric regions of the cell, directly adjacent to Golgi elements and GERL.

The binding and internalization of Au_{16}-hCG appeared to be receptor-mediated because a) Au_{16}-BSA was not observed to bind luteal cells at 4°C, and associated with surface membrane minimally after 90 min., b) internalization of surface associated Au_{16}-hCG did not occur at 4°C, and c) binding of Au_{16}-hCG was blocked by incubation of cells with Au_{16}-hCG in the presence of excess native hCG.

Prior to any labeling experiments the gold complex was tested for the ability to bind the hCG receptor. Au_{16}-hCG was shown to effectively compete with ^{125}I-hCG for binding sites on membranes from corpora lutea, and to bind with an efficiency approximately one magnitude less than that observed for native hCG. In addition, Au_{16}-hCG was shown to elicit progesterone release from luteal cells that was comparable to release stimulated by native hormone.

In an attempt to examine microfilament redistribution concommitant with the endocytosis of hCG, myosin subfragment-1 (S-1) was prepared by chymotryptic cleavage, purified by saturated ammonium sulfate precipitation, and shown to bind specifically to purified F-actin. Microfilaments from resting luteal cells were shown to decorate with S-1 and to be distributed throughout the cytoplasm. Luteal cells incubated with Au_{16}-hCG for 60 min. at 37°C were subsequently labeled with S-1. Microfilaments that were labeled with S-1 were observed to associate directly with areas of the plasma membrane that were occupied by Au_{16}-hCG. Attempts to visualize the organization of microfilaments associated with intracellular organelles labeled with Au_{16}-hCG by decoration with S-1 were unsuccessful. Microtubules were observed to be

numerous along the endocytic pathway. Intermediate filaments appeared to associate directly with coated vesicles containing Au_{16}-hCG and with lysosome like structures filled with gold beads.

In conclusion, Au_{16}-hCG was rapidly internalized by fully differentiated luteal cells along a pathway consistent with that observed during the receptor-mediated endocytosis of a variety of hormones and nutritive substances. We suggest that the initial endosomes observed to accumulate Au_{16}-hCG during endocytosis in vitro are the morphological equivalent to the tenuous processes that are observed to accumulate hormone in vivo. Cytoskeletal elements appeared to be directly associated with surface membranes and with membranes of subcellular organelles involved in the receptor-mediated endocytosis of Au_{16}-hCG. On the basis of these findings we plan to a) determine if the appearance of Au_{16}-hCG in initial endosomes prior to delivery to secondary endosomes is related to hormone and receptor uncoupling, and b) determine whether the repeated structural associations between cytoskeletal elements and organelles involved in the RME of Au_{16}-hCG are related functionally to the endocytic process.

TABLE OF CONTENTS

SECTION		PAGE
I.	Introduction	1
	A. Receptor-mediated Endocytosis	1
	B. RME in the Cultured Fibroblast	2
	C. Fate of the Liqand during RME	5
	D. Fate of the Receptor during RME	5
	E. Cytoskeletal Involvement in RME	7
	F. RME in Luteal Cells	9
	G. Objectives of this Study	11
II.	Materials and Methods	12
	A. Cells	12
	1. Isolation	
	2. Binding Studies	
	B. Experimental Design	13
	1. Au_{16}-hCG Internalization	
	2. Microfilament Decoration of Luteal Cells	
	3. Microfilament Decoration of Luteal Cells Treated with Au_{16}-hCG	
	C. Electron Microscopy	15
	D. Preparation of Au_{16}-hCG and Au_{16}-BSA	16
	1. Colloidal Gold Solutions	
	2. Mean Particle Diameter	
	3. Optimum Protein/Gold Ratio	
	4. Formation of Protein and Gold Complex	
	E. Characterization of Au_{16}-hCG	17
	1. Efficiency of Conjugation Procedure	

2. Au_{16}-hCG Binding to Membranes from Corpora Lutea
3. Au_{16}-hCG Induced Physiological Response

F. Preparation of Myosin Subfragment-1 19

G. Characterization of Myosin Subfragment-1 19

1. SDS Polyacrylamide Gel Electrophoresis (SDS-PAGE)
2. Isolation and Purification of Actin
3. Decoration of F-Actin

III. Results 23

A. Reagents 23

1. Viability and Binding
2. Sizing of Au_{16}-hCG
3. Optimum Protein to Gold Ratio
4. Detection of Unbound hCG during Formation of Au_{16}-hCG
5. Ability of Au_{16}-hCG to Bind the hCG Receptor
6. Au_{16}-hCG Stimulated Progesterone Release
7. Characterization of Myosin S-1

B. Au_{16}-hCG Internalization 41

1. Cells Incubated with Au_{16}-hCG during Incubation at 4°C and at 37°C
2. Cells Incubated with Au_{16}-hCG at 4°C only

C. The Cytoskeleton of Luteal Cells 63

1. Microfilaments in Thin Section
2. Replicas
3. The Cytoskeleton and the Endocytic Pathway

IV. Discussion 77

A. Receptor-mediated Endocytosis of Au_{16}-hCG 77

B. Corroboration of Earlier Reports 79

C. Polarity of Binding 80

D. Initial Endosomes Compared to Receptosomes 80

E. Content of Initial Endosomes 81

F. Secondary Endosomes 83

G. Cytoskeletal Elements and the Internalization of Au_{16}-hCG . . 83

H. Conclusions 85

V. List of References 86

VI. Vita 99

LIST OF FIGURES

FIGURE		PAGE
1.	Binding of ^{125}I-hCG to Luteal Cells	25
2.	Suspension of Au_{16} and Latex Beads	27
3.	Relative Potency of Au_{17}-hCG Binding to Luteal Membranes	32
4.	Au_{16} Stimulated Progesterone Release	34
5.	SDS-PAGE Analysis of Myosin Subfragment-1	37
6.	F-Actin and Myosin Subfragment-1	39
7.	Diffuse Binding of Au_{16}-hCG to Luteal Cell Surfaces at 4°C	42
8.	Binding of Au_{16}-hCG to Luteal Cell Surfaces at 4°C	44
9.	Binding of Au_{16}-hCG to Luteal Cell Surfaces with Excess hCG	44
10.	Binding of Au_{16}-hCG to Luteal Cell Suspensions at 37°C after 30 min	46
11.	Binding of Au_{16}-hCG to Luteal Cell Surfaces at 37°C after 60 min	48
12.	Internalization of Au_{16}-hCG in Coated Pits	50
13.	Internalization of Au_{16}-hCG in Initial Endosomes	52
14.	High Magnification of Initial Endosome	55
15.	Localization of Au_{16}-hCG in Multivesicular Bodies	57
16.	Au_{16}-hCG in MTOC Associated Secondary Endosomes	59
17.	Au_{16}-hCG in Golgi Associated Secondary Endosomes	61
18.	S-1 Decorated Microfilaments in Luteal Cells	64
19.	High Magnification of S-1 Decorated Microfilaments	64
20.	Replica of Luteal Cell Surface	67

21. Replica of Luteal Cell Surface that was Cracked 67

22. S-1 Decorated Microfilaments in Au_{16}-hCG Treated Cells 70

23. S-1 Decorated Microfilaments in Au_{16}-hCG Treated Cells 70

24. Intermediate Filaments and Au_{16}-hCG Labeled Coated Vesicle . . . 72

25. Microtubules and Au_{16}-hCG Labeled Coated Vesicles 72

26. Intermediate Filaments and Au_{16}-hCG Labeled Lysosomes 74

CHAPTER I

INTRODUCTION

A. Receptor-mediated Endocytosis

Receptor-mediated endocytosis (RME) is the term used to describe the integrated transport mechanism by which various ligands bound to receptors on a cell's surface are internalized. This process has been shown to involve the concerted active movement of ligand-receptor complexes within the plane of the membrane to a point of capture and concentration in clathrin-coated membrane regions. Ligands appear to be subsequently internalized in coated vesicles, and to accumulate in a series of smooth surfaced vesicles that mediate the transport of the ligands and associated membrane constitutents to the Golgi elements, lysosomes, or nuclear envelope regions (7,8,9,13,40,41,49,51,52, 56,66,67,71,73,80,91,100,102,103,138,139,140,123,118).

Classes of ligands known to be internalized in such clathrin-coated membrane regions include a) hormones like human chorionic gonadotropin (hCG) (1,5,6,30,31,36,87), 3,5,5-triiodothyronine (32,93) insulin (32,91,90,108,115,33,24, 25,27,16) and, epidermal growth factor (EGF) (18,46,59,60,115,137); b) certain nutrients including low density lipoprotein (LDL) (7,8,9,13,51,52,61,22), transferrin (33,81); and c) other effector molecules such as immunoglobulins (110), asialoglycoproteins (ASOG) (49,130), and α_2 macroglobulin (α_2M) (90,92,80, 102,103,138,139,140,129,40,41,123). The mechanism of action of many virions such as the adenovirus vesicular stomatitis virus (VSV), rheovirus, and Semliki forest virus also involve endocytosis in coated membrane regions (45,63,107,136,89).

The compounds listed above represent only a portion of a growing number of substances that have been observed to enter a cell by a receptor-mediated mechanism, and the process is not always selective for just one macromolecule in a given cell type. Insulin, EGF, and α_2M clustered in common patches and were internalized simultaneously in the same coated structures by the Swiss 3T3-4 cells (91,115). Adenovirus and EGF were also observed to enter KB cells in a common coated pit (46). Of immediate interest recently has been the elucidation of a complex series of subcellular organelles through which one or more ligands are processed following RME.

B. RME in the Cultured Fibroblast

The cultured fibrblast has provided an ideal model system in which to observe the processes employed in the transfer of coated vesicles containing ligand-receptor complexes to golgi or lysosomal regions particularly during the uptake of α_2M. On the basis of these studies, Willingham and Pastan identified specific subcellular organelles involved in the RME of α_2M, and formed a hypothesis to explain the mechanism by which these organelles were formed. To initate RME, α_2M became bound to the cell surface of fibroblasts, a process that took place at 4°C. Upon warming to 37°C, α_2M became concentrated in coated pits, and was believed to be stabilized within the coated pits by a process involving transglutaminase linkages (40,41,102,103,138,139,140). Following completion of the microcapping process, the coated pits appeared to rapidly elongate by extending a smooth membranous process into the cytoplasm. During elongation they lost the ability to accumulate rutheneum red from the extracellular space indicating that they probably were no longer open to it. The cryptic coated regions however remained visible, and were

suggested to be stable structures associated with the plasma membrane. At no time in Willingham and Pastan's work were coated vesicles observed to pinch off from these cryptic coated pits. Instead, a smooth-surfaced bulge was believed to form at the neck of the coated pit into which α_2M-receptor complexes flowed. These smooth-surfaces vesicles underwent saltatory motion until they pulsed their contents through transverse golgi elements and associated lysosomal structures.

Willingham and Pastan termed the smooth-surfaced vesicles "receptosomes" to emphasize their role in RME. Receptosomes were characteristically 200-400 nm in diameter, often exhibiting an electron-lucent vesicular element in addition to intralumenar receptor-ligand complexes. The outer membrane possessed a singular fibrillar plaque on its cytoplasmic surface. Receptosomes did not show appreciable acid phosphatase activity. Receptosomes containing α_2M, transferrin, EGF, VSV, or adenovirus were visualized by light and electron microscopy in fibroblasts active in RME (33,45,91,102,103,138,139).

Recently several groups have identified subcellular organelles in other cell types that share morphological (49,130,99) and biochemical characteristics (49,130,99) of receptosomes observed in cultured fibroblasts. Ligand-asialoglycoprotein receptor complexes were accumulated in peripheral tubules and uncoated vesicles by hepatocytes prior to delivery to Golgi and lysosomal regions. Similarly to the receptosome, these smooth-surfaced vesicles lacked detectible aryl sulfatase activity (49,130). In pancreatic acinar cells, horseradish peroxidase (HRP) was internalized into a series of baso-lateral lysosomes that were morphologically identical to receptosomes (99). Semliki forest virus was

internalized by a receptor-mediated mechanism into a series of intermediate vacuoles that shared biochemical and morphological characteristics with receptosomes (63,136,89).

The concept that smooth-surfaced vesicles participated in the transfer of receptor-ligand complexes from coated membrane regions at the cell periphery to the golgi elements in the cell centrosphere was substantiated by a number of studies (7,8,9,5,6,53,54,102,103,138,139,140). However, the hypothesis that stationary coated pits do not pinch off to form coated vesicles in the cultured fibroblast has been recently challenged (104). The surface membranes of cultured fibroblasts that were actively internalizing cationized ferritin by endocytosis were analyzed by serial section. Utilizing this method, Peterson and Van Deurs repeatedly observed free-floating coated vesicles beneath the plasma membrane. In addition, Peterson and Van Deurs observed coated pits that were continuous with regions of the plasma membrane. Smooth-surfaced membrane that was heavily labeled with ferritin bulged from basal regions of these coated pits. These membrane profiles resembled images of "cryptic" coated pits that were active in the formation of receptosomes (102,103,138,139,140,40,41). Willingham, et. al. described smooth surfaced bulges as the site of receptosome formation, and demonstrated that this compartment was not accessible to rhuthenium red in the extracellular space. However, the serial section analysis (104) indicated that similar images were in fact only cross sections of a highly tortuous surface membrane, and that such images should not be considered as representations of true intracellular space.

C. Fate of the Ligand during RME

The intracellular fate of ligand internalized during RME has been clearly documented in a variety of cell types. LDL, hGH, hCG, EGF, and insulin were observed to accumulate in multivesicular bodies (MVB), or lysosomes, where ligand was degraded to its constituent amino acids (23,7,8,9,51,52,58,71,30,31,36). α_2M, and a variety of lectins were believed to be translocated to the golgi elements prior to delivery to lysosomes (53,54,42,43,66,67,68,101). In contrast, transferrin and cluster glycosides were shown to be rapidly recycled to the extracellular space (81,37). The intracellular fate of the receptor following the internalization of the ligand-receptor complex is less clear.

D. Fate of the Receptor during RME

Several lines of indirect evidence support the hypothesis that ligand challenge leads to formation and internalization of the receptor-ligand complex, followed by the recycling of the receptor to the cell surface. Initially, binding assays using radiolabeled ligand provided estimates of cell surface and intracellular binding capacity during RME. By this method, it was determined that cells were able to internalize 5-30X the ligand that would saturate the total surface binding capacity during continuous exposure to ligand. In addition, these cells were able to maintain a constant binding capacity on the cell surface during continuous RME in the presence of protein synthesis inhibitors (51,52,33,80,141). Initially these observations were interpreted as evidence for an intracellular pool of receptors that replenished internalized receptors during RME. However, it is not clear today whether the receptors that are reinserted into the cells surface are derived from an existing intracellular pool or if the

same receptor that is internalized is reinserted. For example, following trypsin treatment that removed 70% of the surface binding capacity, macrophages regained a full complement of surface binding sites for mannosylglycoprotein one minute after washing and warming to 37°C (121). One interpretation of this study was that the trypsin-altered binding sites were replaced by reinsertion of new binding sites derived from a pre-existing intracellular pool. It is also possible that trypsin masked the binding sites temporarily, and that binding activity was restored following washing and warming to 37°C.

With the recent availability of anti-receptor antibodies, direct evidence of receptor internalization during RME has been provided for the first time. RME of asialoglycoproteins was investigated in an elegant study utilizing antibodies to ASOG, the ASOG receptor, and clathrin visualized by colloidal gold immunocytochemistry. Following RME, ligand-receptor complexes appeared first in coated vesicles, and later in smooth-surfaces vesiculo-tubular structures termed CURL for "Compartment of Uncoupling of Receptor and Ligand". The tubulo-extensions of CURL selectively accumulated receptors, and appeared to transverse golgi elements prior to the subsequent fusion with the cell surface. The body of CURL retained the bulk of the ligand. With time, this structure gained the morphological characteristics of a secondary lysosome. It is of interest that the body of CURL shares morphological and biochemical characteristics with that of the receptosome in the fibroblast (49).

The biochemical prerequisite for ligand-receptor complex uncoupling in vitro has been observed to be a reduction of pH in a variety of systems (49,63,89,96,126,129,21,55). Willingham and Pastan suggested that formation of the smooth-surfaced buldge from the side of a cryptic coated pit in fibroblasts

resulted from a proton pump-activated water uptake into the lumen of the coated pit (102,103,138,139,140). In hepatocytes, a rapid drop in pH was thought to fascilitate receptor and ligand uncoupling in CURL at this early stage in the RME pathway (49). Recently intralumenal pH of smooth-surfaced vesicles containing α_2M internalized during RME has been measured. By recording fluorescence changes that accompanied changes in pH, it was determined that the endocytic vesicles became acidic (pH 4.5-5.0) prior to fusion with any other subcellualr organelles (92,129).

E. Cytoskeletal Involvement in RME

Diffusion alone cannot acount for the rate of transfer of receptor-ligand complexes into coated pit regions (131), or for the rate of intracellular transport of the receptor-ligand complexes to golgi or lysosome regions (102,103,138,139,140). As a result, the cytoskeletal system, and in particular the actin-based microfilament system has been implicated in the internalization process during RME (14,6,3,4,113,131,11,12). Evidence to support this hypothesis includes a) biochemical analysis of plasma membranes from resting cells and cells active in RME (113), b) morphological analysis of isolated membranes or membranes of intact cells (5,6,3,12,11,113), and c) utilization of drug treatments that specifically bind to or alter the cytoskeletal elements (5,6,4,113,35).

Biochemical evidence is accumulating that supports the hypothesis that actin can interact directly with the plasma membrane, and in at least one instance can be considered an integral membrane protein. Isolated plasma membrane fractions from WiL2 cells, analysed by SDS-PAGE were found to contain significant levels of actin, myosin, calmodulin, clathrin, and two high molecular weight proteins that corresponded to the molecular weight of spectrin

(113). Isolated plasma membrane from Swiss 3T3 cells contained actin as a major component that was cytochalasin B resistent. In addition, plasma membrane fractions from 3T3 cells that contained actin were incubated in a buffer designed to solubilize F-actin. Only 70% of the membrane associated actin was liberated. This study was interpreted as evidence that the remaining 30% of the membrane-associated actin represented an integral membrane protein.

In a variety of cell types, actin filaments that were organized into bundles appeared to insert directly into plasma membrane. The organization of membrane associated actin filament bundles is particularly well characterized in the stereocilia of the ear (127,128), and in the intestinal microvilli (95,70). Microfilaments in the microvillus core were observed to be attached at the tip and laterally to the microvillar membrane by 3nm bridges containing -actinin. Other proteins hypothesized mediate actin interaction with plasma membranes or organelle membranes include spectrin, filamen, fodrin, vinculin, fascin, and fimbrin (84,133,131,34,20,88,17).

In order to visualize membrane-associated filaments that were not organized into bundles, it was usually necessary to specifically label the filaments along their length with enzymatically produced fragments of the contractile protein myosin. Heavy meromyosin (HMM) and heavy/meromyosin subfragment-1 (S-1) were observed to assume a characteristic arrowhead configuration upon binding to actin-containing filaments in a variety of cell types (15,35,77,116,131). In addition, polarity of the arrowhead configurations, as indicated by the direction of S-1 binding, correlated with a direction along which it was theoretically possible to generate force (76,15). In most cases,

the polarity of actin-containing filaments that were directly associated with membranes indicated the possibility of force generation toward the cell cytoplasm (15,35,113). The accessory contractile proteins myosin, tropomyosin, troponin were implicated in this process (131).

Recently biochemical and morphological analysis of membranes from cells active in RME has indicated structural and functional association between actin containing filaments and these membranes. In one study, regions of granulosa cell membranes that were occupied by caps of Con-A receptor complexes were selectively isolated and treated with HMM. Actin-containing filaments that decorated with HMM formed an interconnecting meshwork directly beneath the Con-A receptor complexes. Antibodies to actin and myosin were used to localize these two contractile proteins on the plasma membranes of resting granulosa cells and those activly endocytosing Con-A. About one-third more contractile protein appeared to be associated with the membrane of the Con-A cap than on the surface of the cell (35). Alhtough several studies have provided insight into cytoskeletal-membrane interactions during RME in a variety of cells, no study to date has examined the role of cytoskeletal elements during the RME of gonadotropic hormone by luteal cells.

F. RME in Luteal Cells

Receptors may be categorized into two classes according to the function of the corresponding ligand (80). Class I receptors bind molecules that function to transmit a signal, i.e. effectors. Class II receptors bind ligand that is a metabolic requirement or nutrient molecule. In this study, the class of the receptor was correlated with the behavior of the receptor during RME. For example, the LDL receptor (class I) was internalized, recycled to the cell

surface in the presence and absence of bound ligand. In contrast, the hCG receptor (class I) was subject to down regulation following ligand challenge and internalization.

Human chorionic gonadotropin (hCG) and luteinizing hormone (LH) appeared to share a common receptor on the surface of ovarian luteal cells (57,109,110,111,79,29). Differentiated luteal cells were estimated to possess approximately 5×10^4 receptors on the cell surface (87) to which LH or hCG was observed to bind with an affinity in the order of 10^{10} M^{-2} (62,29,110,57). The luteal cell responded to the binding of hCG to its receptor with a complex cascade of events including membrane depolarization, Ca^{2+} and Na^+/K^+ pump activation, cAMP production, and phosphorylation of protein kinases, steroidogenic enzymes, and ribosomes. The acute response to hormonal binding leads in turn to a long term increase in progesterone synthesis and secretion, attended by increased protein synthesis and secretory granule release (1,62,117,114).

Initially it was observed that the binding of hCG to the luteal cell surface led to a desensitization or a down regulation of unoccupied receptors as evidenced by the induction of a refractory period during which cells remained unresponsive to further hormonal stimulation (62,36,10,47,38). The desensitization phenomenon was hypothesized to include an initial reduction of hCG binding capacity that was due to receptor occupancy and lasting 6-12 hrs. This period was followed by a second period characterized by the the loss of binding capacity that was not due to receptor occupancy. Furthermore, Harwood found that the occupancy of only 1% of the receptors for hCG led to a down regulation of the total receptor population by 24 hours (62).

To understand the mechanism involved in receptor desensitization resulting from hormonal challenge it was necessary to elucidate the fate of the receptor-ligand complex during RME in luteal cells (36). Unfortunately, a method of specifically labeling receptors along the cell surface is unavailable to date, i.e. an antibody to the hCG receptor.

G. Objectives of this Study

In this study we utilized a well characterized probe, Au_{16}-hCG, in order to determine the fate of the receptor-ligand complex during RME. We provide evidence supporting the hypothesis that hormone was internalized in coated vesicles that transferred their contents to secondary lysosomes or MVB. In addition, we provide new evidence that Au_{16}-hCG was retained in a series of smooth-surfaced endosomes prior to transfer to the vicinity of the golgi-GERL and secondary lysosomes. Although RME has been studied extensively in cultured cell lines, this study represents an effort to clarify the mechanisms employed by large epithelial cell types during RME of hormone.

CHAPTER II

MATERIALS AND METHODS

A. Cells

1. Isolation

Suspensions of enzymatically dissociated luteal cells were prepared according to Simmons et. al. (1975) with modifications. Mid-cycle porcine ovaries were collected from a local slaughterhouse in Locke's media (154 mM NaCl, 5.5 mM KCl, 2.2 mM $Cacl_2$, 3 mM Na_2HPO_4-NaH_2PO_4, 10 mM glucose, pH 7.0) at 4°C. For each separation, approximately 12 corpora lutea were excised from ovaries, separated from connective tissue capsules, and minced with a razor blade for 5 minutes over ice. The resultant 5 grams tissue mince was rinsed in Locke's media and divided between 5 incubation flasks. Collagenase (Sigma, Type IA) at 2000 units per gram tissue mince was suspended in 10 ml. Locke's media per gram tissue, and divided equally between incubation flasks. The mixture was ventilated with air/5% CO_2, and incubated for 1 hr. at 37°C with medium shaking. After 1 hr., the digest was pelleted at 250 x g for 10 min., rinsed twice in Locke's media, and resuspended in 50 ml. fresh Locke's containing 2000 units high purity collagenase (Advance Biofacture ABC Form TD-B) per gram tissue. After 30-45 min. of incubation at 37°C, the digest was washed 5 x in Locke's to remove all enzyme and large connective tissue masses. Single cells were resuspended in 5 ml. RPM-1 (GIBCO), and layered onto a bovine serum albumin (BSA) gradient of 3, 5, and 7% BSA (Sigma, Fraction V) in Eagles, pH 7.3. Cells were separated at unit gravity for

1 hr. at 25°C. The 7% layer and adjacent half of the 5% layer were collected and centrifuged at 250 x g for 10 min. to pellet a highly purified population of single luteal cells.

Cell viability was determined by trypan blue dye exclusion (106). Cell number was calculated in a Neubauer Counting Chamber. Cells were rinsed in media to remove BSA, and incubated at 37°C for 1-3 hrs. prior to any experiments.

2. Binding Studies

Human chorionic gonadotropin (hCG) (CR121, Dr. Canfield, Columbia) was radioiodinated by the lactoperoxidase method (105). Aliquots of 700,000 cells in 1.0 ml. media were incubated with 2.5 x 10^6 cpm ^{125}I-hCG for 15, 30, 60, and 120 min. at 37°C in the presence and absence of 100 micrograms native hCG. Following addition of 3 ml cold phosphate buffered saline (PBS) (0.1M Na_2HPO_4-NaH_2PO_4, 0.05 M NaCl), the cells were pelleted at 1700 x g for 15 min. at 4°C. The supernatant was aspirated to remove unbound ^{125}I-hCG, and bound radioactivity in the cell pellet was determined in a Beckman 4000 gamma counter.

Cells were preincubated at 37°C for 1-3 hrs., rinsed, and resuspended in Eagles media. Aliquots were transferred to Eppendorf tubes for the following experiments:

B. Experimental Design

1. Au_{16}-hCG Internalization

Au_{16}-hCG (16 micrograms in 300 ul. Buffer A[II]: 0.15 M NaCl, 50 mM Tris-HCl, pH 7.0 with .0006% M Carbowax 20-M, Union Carbide) was added

to 1.0 x 10^6 cells suspended in 500 ul. media. All groups were incubated at 4°C for 2.5-4 hrs., and warmed to 37°C for 3, 5, 10, 15, 30, 45, 60, and 90 min. In some experiments cells were incubated with Au_{16}-hCG for 4 hrs. at 4°C, rinsed, and incubated in media during all timepoints following warming to 37°C. Incubations were terminated by rinsing cell pellets with media and followed by fixation in 2% glutaraldehyde in 0.1 M sodium cacodylate, pH 7.3 containing 5% sucrose, overnight at 4°C. Control groups included cells incubated with 300 ul. Au_{16}-BSA, or with 300 ul. Au_{16}-hCG in the presence of native hCG, with Buffer A^1, or media alone.

2. Microfilament Decoration of Luteal Cells

Cells were treated with absolute ethanol at 0°C for 2 min., rinsed briefly in media, and incubated with myosin subfragment-1 (S-1) at a concentration of 2-3 mg/ml in standard salt buffer (0.1 M KCl, 1.0 mM $MgCl_2$, 0.2 M sodium phosphate, pH 7.0) (76), or in stabilization buffer (0.1 M PIPES, pH 6.9, containing 1.0 mM EGTA, 2.5 mM $MgCl_2$, and 2.5% DMSO) (14), for 20 min. at 25°C. Cells were rinsed in stabilization buffer and fixed overnight in 2% glutaraldehyde in 0.1 M sodium cacodylate, 4.5 mM $CaCl_2$, 0.2% tannic acid. Control groups included cells incubated in stabilization buffer without S-1, and cells incubated with S-1 without prior ethanol treatment. In other experiments, 100,000 cells in 300 ul. media were allowed to attach to poly-L-lysine coated coverslips for 2.5 hours at 37°C. Cells were cracked open using a sandwich coverslip method described by Batten et al., (14) where coverslips were allowed to settle onto the apical regions of attached luteal cells for 15 min. at 37°C. Coverslips were removed with forceps to crack open cells that were subsequently rinsed and fixed, or incubated with S-1 (2 mg/ml) in stabilization buffer

containing 2 mM phenylmethyl sulfonyl fluoride (PMSF) for 5 min. at 25°C, followed by fixation overnight at 4°C.

3. Microfilament Decoration of Luteal Cells Treated with Au_{16}-hCG

Cells incubated with 20 ug. Au_{16}-hCG for 2.5 hrs. at 4°C and 1 hr. at 37°C were rinsed in media, treated with absolute ethanol at 0°C for 2 min., and incubated with S-1 in stabilization buffer (2-3 mg/ml), rinsed, and fixed overnight in 2% glutaraldehyde, 0.1 M sodium cacodylate, 4.5 mM $CaCl_2$, and 0.2% tannic acid (15,50). Cells designated as controls received Au_{16}-hCG incubation and ethanol treatment as above, and were fixed overnight without prior incubation in S-1.

C. Electron Microscopy

Cells fixed overnight at 4°C were rinsed in 0.1 M sodium cacodylate buffer, pH 7.0 containing 5% sucrose, postfixed in 1% OsO_4 in 0.1 M sodium cacoylate for 30 min. at 25°C, stained en bloc by saturated uranyl acetate in ethanol for 1 hr. at 25°C, and dehydrated through an ethanol series. Cell pellets were embedded in Epon, thin-sectioned on a Porter Blum MT-2B ultramicrotome, post stained with uranyl acetate and lead citrate, and viewed on a Hitachi H-600 at 75 kV. Cells that were attached to coverslips and cracked open were fixed overnight at 4°C, rinsed in cacodylate buffer, postfixed in cacodylate buffered O_sO_4 (1%) for 5 min., and dehydrated through the ethanol series. Following critical point drying, cells were rotary shadowed with platinum-carbon (Polysciences #1039, 1 inch wrapped around a carbon rod). Replicas were placed in concentrated HF until the glass coverslip dissolved or the replica floated free from the coverslip. Replicas were cleaned of remaining

tissue in clorox, washed twice with dH_2O, and broken with forceps to be picked up on formvar coated 300 mesh copper grids. The clorox and the dH_2O washes contained 0.1% Photo-Flo 200 (Kodak) to reduce surface tension. Replicas were viewed by TEM in a Hitachi H-600 at 75 and 100 kV.

D. Preparation of Au_{16}-hCG and Au_{16}-BSA

1. Colloidal Gold Solutions

Colloidal gold solutions were prepared according to Horisburger, (73,74) as follows: 200 ml dH_2O was heated under reflux to which 1% sodium citrate (6-10 mls.) and 4% $HAuCl_4$ (0.5 mls) was added. The clear solution turned grey, black, purple, and then red over a 2 min. interval, and was boiled under reflux for 30 min. to ensure complete reduction of $HAuCl_4$.

2. Mean Particle Diameter

Mean gold particle diameter was determined by examination of transmission electron micrographs of a gold solution and latex beads of a known diameter. Gold and latex beads were mixed in a 2:1 ratio for several min. and allowed to settle onto formvar coated, carbon coated copper grids for 2 min., followed by negative stain with 1% uranyl acetate in dH_2O.

3. Optimum Protein/Gold Ratio

The optimum protein concentration needed to stabilize gold solutions was determined by monitoring absorbance loss at 550 nm upon flocculation induced by the addition of NaCl as described by Horrisburger and Rosset (75). Gold solution (2.5 mls) was added to serial dilutions of hCG or BSA in 0.5 ml. of 5.0 mM NaCl. Absorbance readings were recorded before and after addition

of 10% NaCl (1.0 ml.). Flocculation was also judged visually by a color change from orange-red to lavender or grey that accompanied loss in absorbance at 550 nm.

4. Formation of Protein and Gold Complex

hCG (3.0 mg) or BSA (4.1 mg) was suspended in 2.0 ml 5.0 mM NaCl in a plastic container. The pH of the gold solution to be used for conjugation was adjusted to a pH slightly basic of the isoelectric point of the protein, pH 4.0 for hCG, and pH 4.9 for BSA (48). The gold solution (50 ml) was added to the protein solution, shaken manually for 2 min., and stabilized with addition of 1% Carbowax 20-M (30 ul.). The protein-gold conjugate was neutralized with 0.2 N K_2HCO_3, and pelleted at 28,000 x g for 30 min. at 4°C. The supernatant was carefully aspirated, and the pellet containing the gold-protein conjugate was washed with 50 ml buffer A^{I} (Buffer A containing .001% Carbowax 20-M), and twice again with 50 ml buffer A^{II} (Buffer A with .0005% Carbowax 20-M). The pellet was resuspended in 5 or 10 ml buffer A^{II} and used immediately or stored at 4°C away from light.

E. Characterization of Au_{16}-hCG

1. Efficiency of Conjugation Procedure

hCG (2 mg.) was conjugated to 34 mls of gold solution as described above in the presence of trace ^{125}I-hCG (2-5 x 10^5 cpm). Aliquots from each of the supernatants following the washes, and the final pellet of Au_{16}-hCG were counted in a Beckmann 4000 gamma counter.

2. Au_{16}-hCG Binding to Membranes from Corpora Lutea

Au_{16}-hCG and native hCG were allowed to compete with ^{125}I-hCG for hCG receptors on membranes in a homogenate of porcine corpora lutea as follows: mid-cycle corpora lutea (CL) were excised from porcine ovaries minced slightly with a razor blade, and homogenized in a Dounce homogenizer. The homogenate was centrifuged at 400 x g for 15 min. at 4°C, and the supernatant collected and spun at 30,000 x g for 30 min. at 5°C to pellet a crude membrane preparation. Protein concentration in the CL membrane preparation was determined according to Bradford (19). A preliminary binding assay that measured ^{125}I-hCG binding to serial dilutions of membrane preparation was used to determine the optimum volume of CL membrane needed for subsequent assays. CL membrane (300 ul.) and serial dilutions of Au_{16}-BSA, Au_{16}-hCG, or native hCG were incubated in the presence of ^{125}I-hCG (5 x 10^4 cpm) in a total reaction volume of 550 ml for 3 hr. at 37°C. The reaction was terminated by addition of 3 ml cold PBS, and the membrane pelleted at 17,000 x g for 15 min. at 4°C. The supernatant was aspirated and bound radioactivity in the membrane pellet was determined in a Beckman 4000 gamma counter.

3. Au_{16}-hCG Induced Physiological Response

Dissociated luteal cells treated with Au_{16}-hCG (16 ug) for 1 hr. at 37°C were pelleted and the media assayed for progesterone by radioimmunoassay (105). Media surrounding cells for 1 hr. in the absence of Au_{16}-hCG was also assayed for progesterone.

F. Preparation of Myosin Subfragment-1

Chymotryptic myosin subfragment-1 (S-1) was prepared according to the methods of Detmers et al. (39) and Weeds and Taylor (135) as follows: 150 mg. myosin (Sigma, rabbit skeletal in 0.6 M KCl, 50% glycerol) at 4.5 mg/ml was precipitated in 360 ml dH_2O and pelleted at 10,000 x g for 10 min. at 4°C. The pellet was resuspended in digestion buffer (60 mM NaCl, 500 mM EDTA, 20 mM sodium phosphate, 0.2 mM diothiothreitol (Kodak), pH 7.0 to a concentration of 8-10 mg/ml. -chymotrypsin (Sigma, TLCK treated) was resuspended in 0.5 ml digestion buffer at a concentration of 0.5 mg per ml. myosin solution at 10 mg/ml. The enzyme was stirred into the myosin solution and the digestion allowed to proceed for 20 min. at 25°C with slow stirring. The enzyme was neutralized by addition of 150 ul. 100 mM PMSF in 70% ethanol to a final concentration of 0.1 mM (Johnson and Taylor, 1978). After removal of the rods at 10,000 x g for 10 min., the supernatant was precipitated with ammonium sulfate at concentrations of 45, 50, 55, and 60%. Each precipitate was allowed to equilibrate for 30 min. at 4°C, and collected by centrifugation at 10,000 x g for 10 min. Pellets were resuspended in equal volume of standard salt solution (0.1 M KCl, 1.0 mM $MgCl_2$, 0.2 M sodium phosphate, pH 7.0) and dialyzed against 5 changes of standard salt solution over 3 days at 4°C.

G. Characterization of Myosin Subfragment-1

1. SDS Polyacrylamide Gel Electrophoresis (SDS-PAGE)

Ammonium sulfate precipitates were analyzed with SDS-PAGE according to the method of Weber and Osborn (132) and Weeds and Pope (134).

Polyacrylamide gels at 6-10% were made from a stock solution of 30% acrylamide, 0.8% bis-acrylamide (Biorad). Gels were polymerized with ammonium persulfate and N,N,N,N-tetramethylethylenediamine in the presence of 0.1% sodium dodecyl sulfate (Sigma, lauryl sulfate) in 0.1 M sodium phosphate, pH 7.2. Concentration of protein in the fractions from saturated ammonium sulfate analysis was determined according to Bradford (1976). Electrophoresis was performed in 12.5 mm x 5.5 mm glass tubes (Biorad) at 5-10 mAmp/tube overnight in a running buffer of 0.1 M phosphate pH 7.2 containing 1% SDS. Ammonium persulfate (50 ug) or a series of high molecular weight standards (Biorad) were combined with an equal volume of sample buffer containing 10% SDS, 1% β-mercaptoethanol, 0.1% bromophenol blue, and 9% glycerol. Frozen or fresh protein samples were boiled for 2 min. prior to loading onto gels. Gels were removed from tubes by expulsion with a syringe filled with chilled dH_2O. Gels were stained overnight in 500 ml. of a solution containing 1.25 g. Coomassie Brilliant Blue R-250 (Kodak), 45% methanol (v/v) and .01% glacial acetic acid (v/v), and destained for 2 days in a solution containing .075% acetic acid and .05% methanol (v/v).

All protein fractions suitable for decoration of actin-containing filaments as determined by SDS-PAGE analysis were stored in standard salt soution, and 50% glycerol at 0°C.

2. Isolation and Purification of Actin

A cardiac muscle acetone powder was prepared according to Carsten and Mommaerts (1963) as follows: 3-5 porcine hearts were cut into 2.5 cm cubes, cleaned of connective tissue, and stored in dH_2O on ice overnight. The tissue and dH_2O was minced in a waring blender and extracted with the following

series: 0.1 M KCl (3:1 w/v), .05 M $NaHCO_3$ (3:1 w/v), 1 mM EDTA (10:1 w/v), two dH_2O washes, and two acetone extractions at 0°C (2:1 and 1:1 w/v). The tissue mass was stirred in each extract for 20 min. at 4°C and filtered through 2 layers of cheesecloth. The final tissue residue was dried overnight, ground into a fine powder, and stored at 4°C to be extracted within 2 weeks. A 900 ml. tissue mince from 4 porcine hearts yielded 20 grams acetone powder.

Actin was extracted from the acetone powder according to Spudich and Watt (120) as follows: 10 g. acetone powder were extracted with 200 ml buffer A (2.0 mM Tris-HCl, 0.2 mM ATP, 0.5 mM -mercaptoethanol, 0.2 mM $CaCl_2$, pH 8.0) for 30 min. at 4°C with gentle stirring, and filtered under vacuum through course filter paper (Whatman). The residue was extracted again in buffer A, and refiltered. The two filtrates were combined and clarified by centrifugation at 10,000 x g for 1 hr. at 4°C. Actin was polymerized in .05 M KCl, 2 mM $MgCl_2$, pH 7.0 for 2 hr. at 4°C, and in 0.6 M KCl for an additional hour at 4°C, and pelleted at 80,000 x g for 3 hrs. Pellets of F-actin were resuspended in 20 ml. buffer A and dialysed against buffer A for 3 days or until the pellet was solubilized to G-actin. The concentration of protein in the soution of G-actin was determined according to Bradford (19). The purity of G-actin and F-actin was estimated by using SDS-PAGE. 10 g. of acetone powder of cardiac muscle yielded 122.5 mg. pure G-actin that was stored at 3.5 mg/ml in buffer A at 4°C, or in buffer A and 50% glycerol at 0°C.

3. Decoration of F-actin

G-actin was dialyzed against standard salt solution to form F-actin. Myosin S-1 (4 mg/ml in standard salt solution) and F-actin (2 mg/ml in standard salt solution) were combined in an optimum ratio of 5.2 to 1.0 as determined

by Szentgyorgy (125) for 5 min. at 25°C or overnight at 4°C. S-1 decorated F-actin was transferred onto holey formvar coated, carbon coated, 300 mesh copper grids. Grids were rinsed with standard salt, followed by a solution containing cytochrome C oxidase and .001% amyl alcohol, and negatively stained with 1% uranyl acetate in dH_2O. Control preparations included 0.2 mM ATP in the buffer during the incubatin of F-actin with S-1 (94).

CHAPTER III

RESULTS

A. Reagents

Before performing the studies on the internalization of Au_{16}-hCG by the dissociated luteal cells, it was first necessary to (1) determine the viability of the luteal cell suspensions, and test for the ability of the cells to bind hCG to receptors on the cell surface following each enzymatic dissociation. The optimum ratio of protein and gold solution was determined (2), the gold complex was monitored for the presence of significant levels of unbound hCG (3), and the particle diameter of the gold complex was determined (4). Au_{16}-hCG was tested for the ability to competitively bind luteal cell membranes compared to that of native hCG (5), and induce progesterone secretion from luteal cell suspensions (6). The purity of the myosin S-1 was determined using SDS-PAGE (7). Myosin S-1 was then tested for the ability to bind actin containing filaments in preparations of purified F-actin (8) that were negatively stained.

1. Viability and Binding

A typical enzymatic dissociation of 5 g. corpora lutea yielded 2.0-5.0 x 10^7 cells that were greater than 90% viable. The highly purified luteal cell suspensions were essentially devoid of cellular debri, blood cells, or cells smaller than 10 um. in diameter. The population of isolated cells represented a mixture of small luteal cells, 10-20 um. in diameter, and large luteal cells, 20-50 um. in diameter.

Cells bound ^{125}I-hCG half maximally by 15 min. at 37°C. Binding reached a plateau by 45 min. at 37°C, and was displaced almost entirely by the presence of native hCG in 100 fold excess (Fig. 1).

2. Sizing of Au_{16}-hCG

Latex beads of known diameter (88 ± 8 nm) were mixed with the gold solution or the gold-protein complex to enable determination of the mean gold particle diameter. At least 250 particles were measured from images of negatively stained preparations of the gold and latex bead mixture (Fig. 2). By this method, the mean gold particle diameter was calculated to be 16 ± 1.5 nm. On the basis of this determination, gold particles were referred to as Au_{16} and the complexes as Au_{16}-hCG or Au_{16}-BSA. Neither of the proteins were able to be visualized on the surface of the gold particles using the negative stain preparations.

3. Optimum Protein to Gold Ratio

The optimum protein to Au_{16} ratio determined by stabilization against NaCl induced flocculation was 0.1 mg hCG to 5 ml Au_{16} solution, and 1 mg BSA to 5 ml Au_{16} solution (Table 1). Proteins were added in 10% excess of the optimum concentration determined by this method.

4. Detection of Unbound hCG during Formation of Au_{16}-hCG

A small amount of ^{125}I-hCG (2 ng at 260,000 cpm) was included in a typical conjugation procedure in order to monitor the amount of hCG that bound to Au_{16}, and to ensure that no unbound hCG remained in the final solution of Au_{16}-hCG (2). The percent recovery of tracer in all pellet washes, and the final pellet are presented in Table 2. It was calculated that 20% of

Figure 1: Binding of ^{125}I-hCG to Luteal Cells. Binding of ^{125}I-hCG to suspensions of porcine luteal cells achieved half maximal values after 15 min., and appeared to be saturated by 60 min. at 37°C. Binding in the presence of excess native hCG (Δ---Δ) was subtracted from binding in the presence of ^{125}I-hCG alone (o--o) in order to calculate specific binding (●--●).

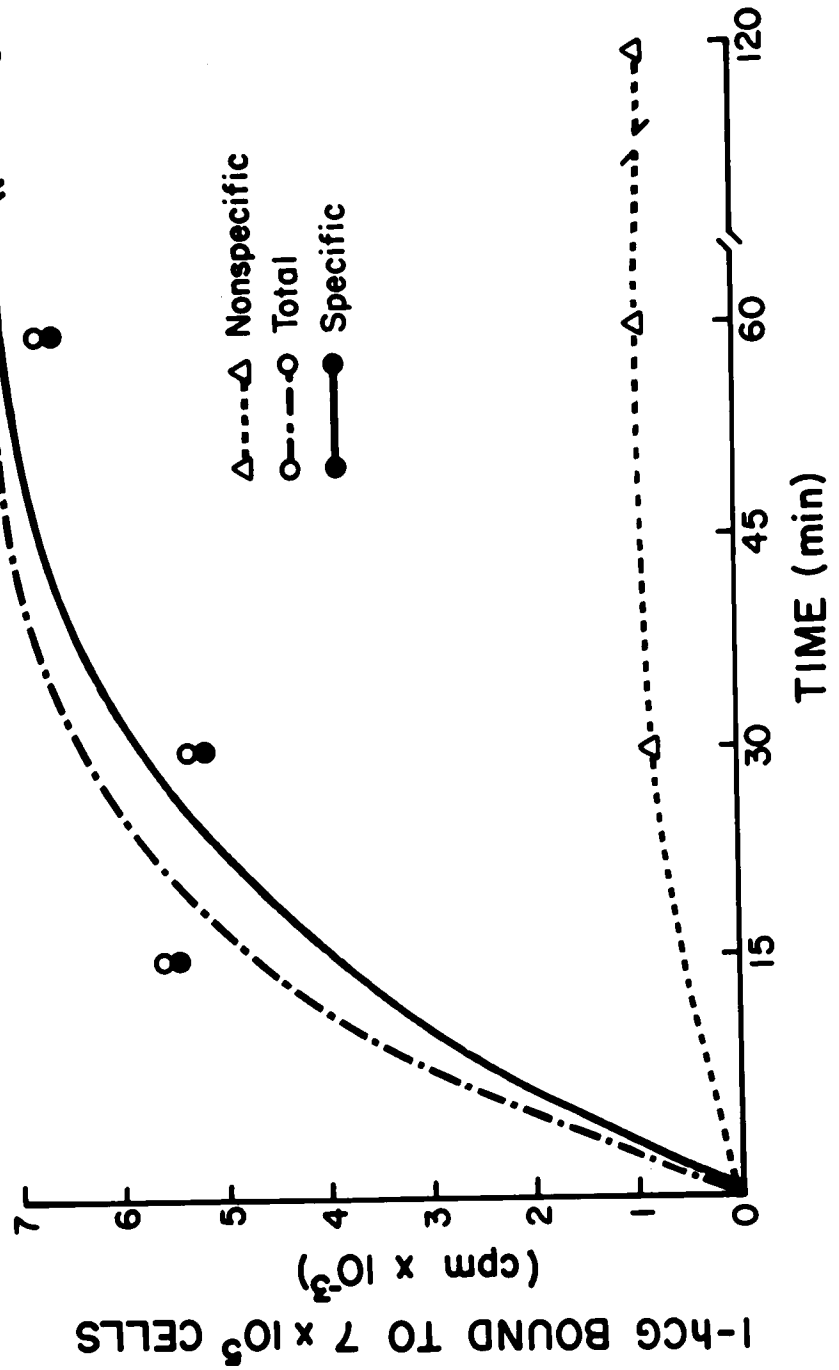

Nonspecific
Total
Specific
TIME (min)
0
15
30
45
60
120
1
2
3
4
5
6
7
(cpm x 10³)
I-hCG BOUND TO 7 x 10⁵ CELLS

Figure 1

Figure 2: Suspension of Au_{16} and Latex Beads. Electron micrograph of a negatively stained preparation of colloidal gold, prepared by the reduction of $HAuCl_4$ by sodium citrate, and latex beads of a known diameter (88 ± 8 nm). Mean diameter of the gold beads was calculated to be 16 ± 1.5 nm (X115,000).

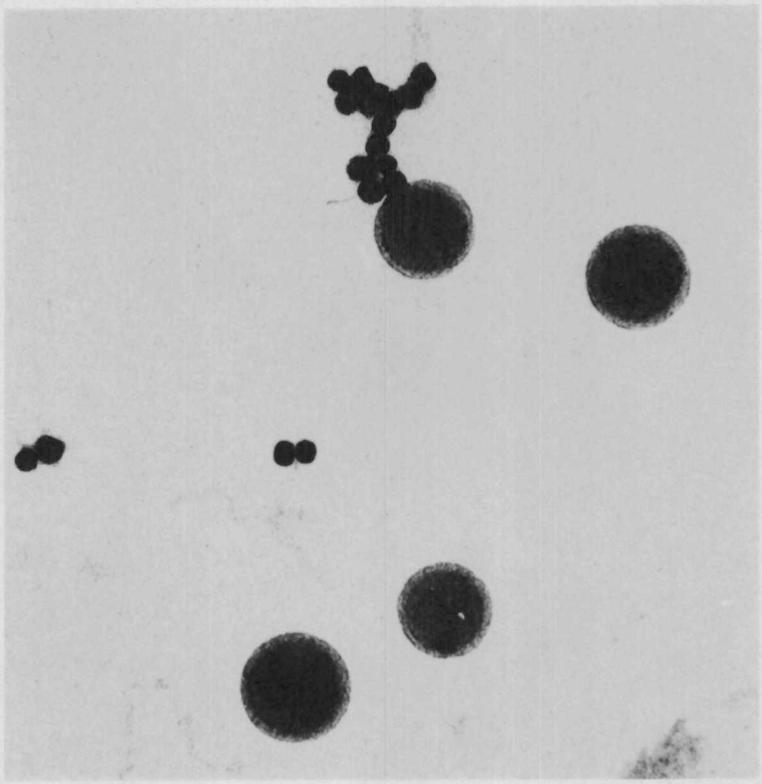


Figure 2

Table I. Optimum Protein Concentration Necessary for the Formation of Au_{16}-hCG and Au_{16}-BSA.

Protein Concentration (ug)		Absorbance (nm)	Color Prior	Color
hCG	BSA	Following 10% NaCl	to 10% NaCl	Following 10% NaCl
1000.0		.544	Red	Red
500.0		.549	Red	Red
50.0		.544	Red	Violet
5.0		.414	Red	Purple
0.5		.239	Red	Grey
0.05		.234	Red	Grey
0.0		.239	Red	Grey
	1000.0	.291	Red	Red
	100.0	.111	Red	Violet
	10.0	.019	Red	Grey
	1.0	0	Red	Grey
	0.0	0	Red	Grey

Table 2. Detection of Unbound hCG During Conjugation.

Supernatant/Pellet	^{125}I-hCG(cpm)	Recovery of Tracer(%)	Total hCG(ug)	Volume of Supernatant(ml)	hCG in 300 ul Dose (ng)
Supernatant No. 1	136620	67.73	1354.6	30	13,500
Supernatant No. 2	8016	3.97	79.4	63	378
Supernatant No. 3	1.512	0.75	15.0	18	250
Supernatant No. 4	1.258	0.62	12.4	21	170
Pellet	5.4144	26.84	536.8	10	16,100*

*16 ug in 300 ul was used to stimulate 1.5 x 10^6 cells during a typical experiment.

the hCG added during one labeling procedure was recovered in the final Au_{16}-hCG pellet at an estimated ratio of 182 hCG molecules per gold granule. The final gold complex used for all binding experiments contained approximately 9 pg unbound hCG in the 300 ul aliquot used to stimulate 1.0×10^6 cells.

5. Ability of Au_{16}-hCG to Bind the hCG Receptor

Au_{16}-hCG and Au_{16}-BSA were allowed to compete with ^{125}I-hCG for LH/hCG receptors in a luteal membrane preparation to determine to what extent the biological activity of the Au_{16}-hCG was altered. After comparing the binding of Au_{16}-hCG to that of native hCG, it was estimated that the ED_{50} of Au_{16}-hCG is approximately one magnitude lower than native hCG (Fig. 3). Conversely, in the control preparations, the Au_{16}-BSA did not displace the binding of ^{125}I-hCG.

6. Au_{16}-hCG Stimulated Progesterone Release

Au_{16}-hCG was tested for the ability to elicit a physiological response as determined by its ability to stimulate progesterone secretion from luteal cells. Media containing 1.0×10^6 cells incubated in the presence of Au_{16}-hCG was assayed for progesterone by radioimmunoassay. Progesterone secretion in response to Au_{16}-hCG and basal progesterone release in the absence of hCG is shown in Fig. 4. The amount of progesterone (180 ng) released into the incubation media after 120 min. was comparable to values for progesterone secretion obtained from luteal cells stimulated by native hCG (119,82,29,44).

As a control, cells were incubated in the presence of Au_{16}-BSA and the incubation media assayed for progesterone as above. After 120 min., 48 ng of progesterone was present in the incubation media from cells treated with

Figure 3: Relative Potency of Au_{17}-hCG Binding to Luteal Membranes. Comparison of the ability of Au_{17}-hCG (o-o) and native hCG (●-●) to compete with ^{125}I-hCG for binding sites on membranes from porcine corpora lutea. The formation of the gold-hCG complex appears to reduce the ability of Au_{16}-hCG to bind the receptor by approximately one order of magnitude of that observed for native hCG. Au_{17}-BSA was not able to compete for hCG binding sites (Δ--Δ).

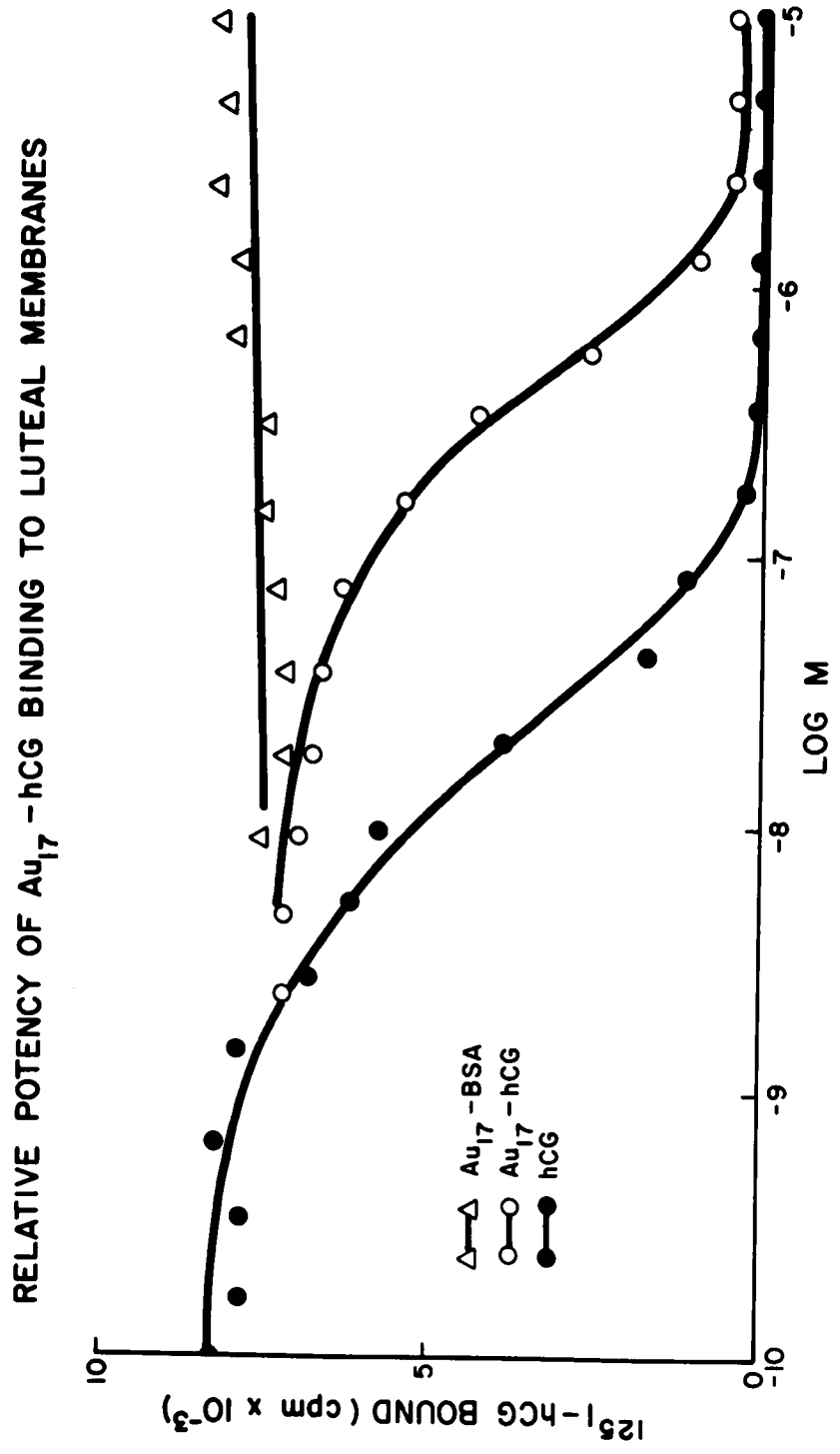

RELATIVE POTENCY OF Au_{17}-hCG BINDING TO LUTEAL MEMBRANES
^{125}I-hCG BOUND (cpm x 10^{-3})
10
5
0
-10
-9
-8
-7
-6
-5
LOG M
Au_{17}-BSA
Au_{17}-hCG
hCG

Figure 3

Figure 4: Au_{16} Stimulated Progesterone Release. Release of progesterone by suspensions of luteal cells incubated with Au_{16}-hCG (□--□) was determined by radioimmunoassay. Au_{16}-hCG stimulated progesterone release was 3 fold over of basal progesterone release (□--□) that was measured in the absence of hormone.

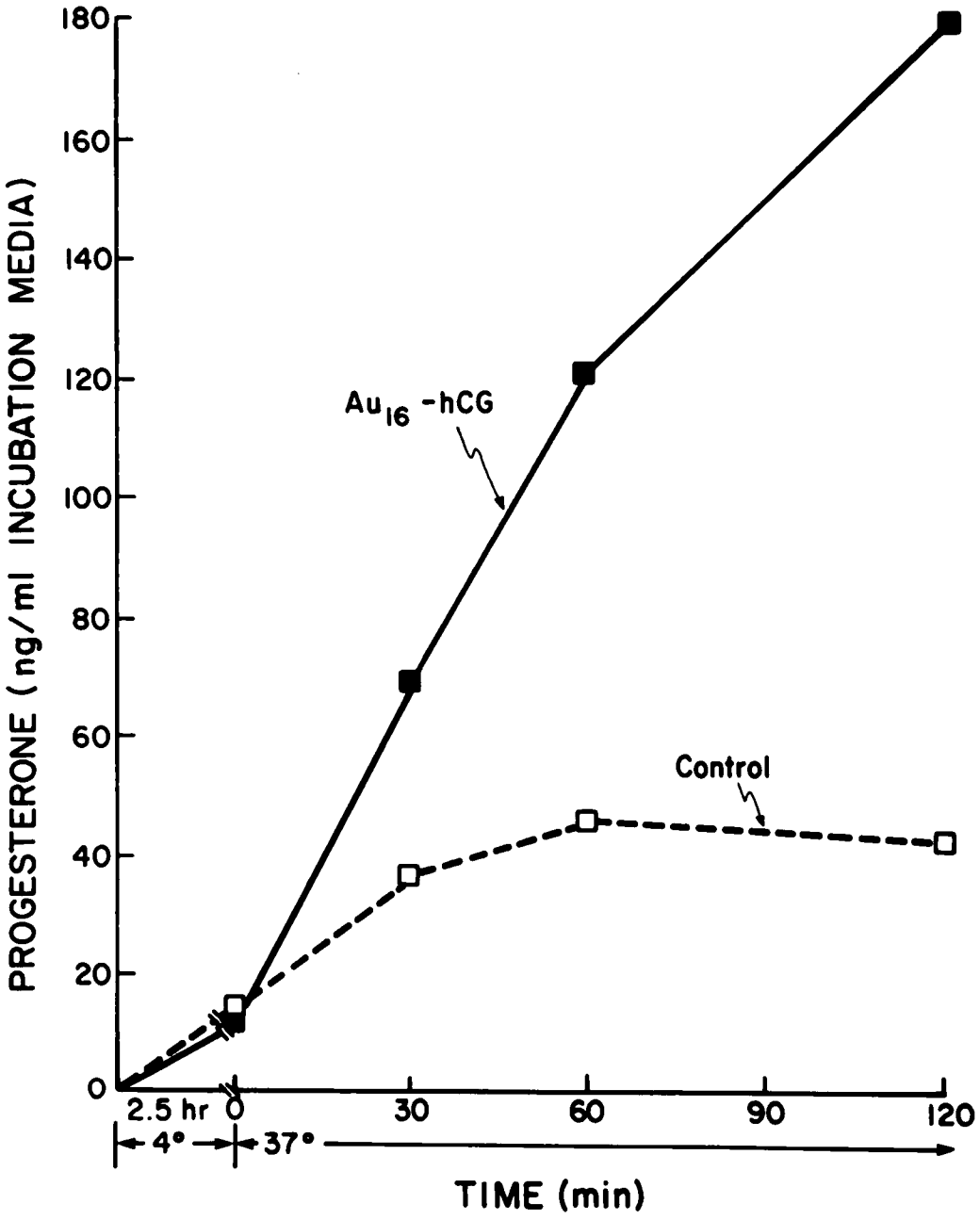

180
160
140
120
100
80
60
40
20
0
PROGESTERONE (ng/ml INCUBATION MEDIA)
Au16 -hCG
Control
2.5 hr
0
30
60
90
120
4°
37°
TIME (min)

Figure 4

Au_{16}-BSA. This progesterone level was comparable to basal progesterone secretion (42 ng) observed from cells incubated in the absence of hormone.

7. Characterization of Myosin S-1

SDS-polyacrylamide gel electrophoresis was used to estimate the molecular weights of proteins present in fractions of the myosin digest that precipitated at 45, 50, 55, and 60% concentrations of saturated ammonium sulfate (SAS). The precipitates were compared to a series of high molecular weight standards, undigested myosin, and F-actin. The fractions precipitated at 50, 55, and 60% SAS contained significant amounts of a protein of a molecular weight of 90,000 D that was identical to the molecular weight reported for myosin S-1 (86,134,85,122) (Fig. 5).

All fractions containing a protein with the molecular weight of myosin S-1 were tested for the ability to bind purified F-actin in suspension. Filamentous structures with the characteristic arrowhead configuration were observed by the decoration of F-actin with the 50 and 55% SAS precipitate, but not by the 60% SAS precipitate. F-actin incubated with myosin S-1 in the presence of 0.2 mM ATP did not assume the arrowhead configuration (Fig. 6). The specificity of the decoration of actin-containing filaments in luteal cells treated with the 55% fraction was determined by comparison with images of decorated F-actin in suspension. Both preparations produced arrays of filamentous structures with discernible arrowhead configurations and recognizable polarity.

Figure 5: SDS-PAGE Analysis of Myosin Subfragment-1. SDS-PAGE of the products from the chymotryptic digestion of skeletal muscle myosin. Molecular weight standards include β-galactosidase, 116 K; phoshorylase-B, 93K; bovine serum albumin, 66K; and ovalbumin, 45K. Lane A: undigested myosin; Lane B: 45% saturated ammonium sulfate (SAS) precipitate; Lane C: 50% SAS precipitate; Lane D: 55% SAS precipitate; Lane E: 60% SAS precipitate; Lane F: purified cardiac muscle actin. Lanes 1-5 represent 55% SAS precipitates from 5 separate chymotryptic digestions to illustrate a) variability in proteolytic fragments between digests, and b) the presence of significant levels of myosin subfragment-1 in 55% SAS precipitates from each digestion. Heavy chains of myosin subfragment-1 constitute the major band at approximately 90K.

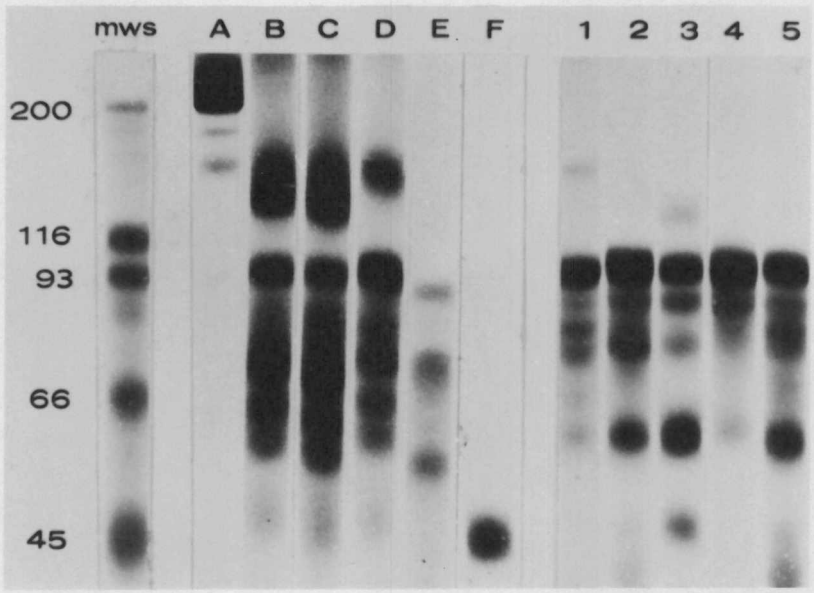


Figure 5

Figure 6: F-Actin and Myosin Subfragment-1. All panels represent electron micrographs of filaments that were negatively stained with uranyl acetate. Top left: Purified cardiac muscle F-actin. Top right: F-actin decorated with myosin S-1 and HMM from a 50% SAS precipitate (polarity of binding is indicated with arrow). Bottom left: F-actin decorated with S-1 from a 55% SAS precipitate (polarity of binding is indicated by arrow). Bottom right: F-actin incubated with a 55% SAS precipitate in the presence of 0.2 M ATP. No decoration was observed (X50,000).

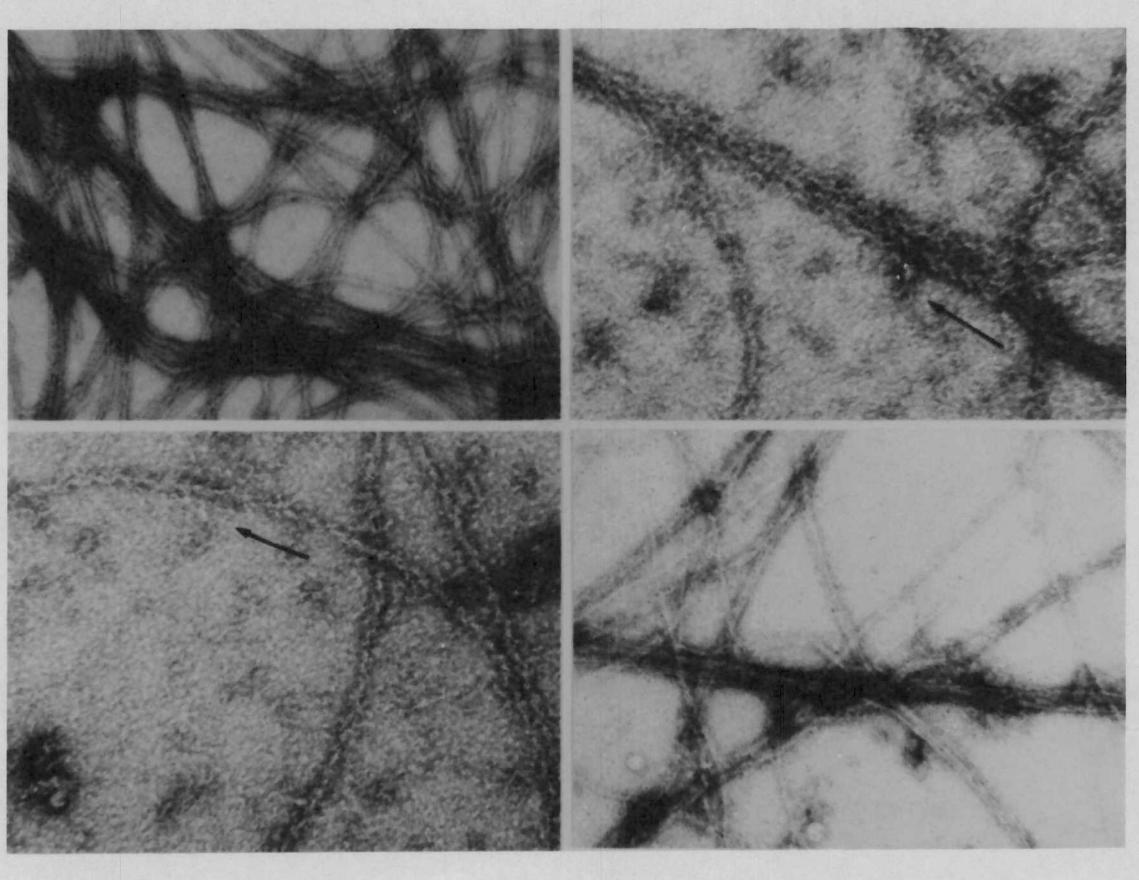


Figure 6

B. Au_{16}-hCG Internalization

1. Cells Incubated with Au_{16}-hCG during Incubation at 4°C and at 37°C

After enzymatically dissociated luteal cells were incubated with 16 ug Au_{16}-hCG for 4 hrs. at 4°C, gold particles were localized initially on cytoplasmic folds and microvilli along the cell surface (Fig. 7,8). The majority of the gold particles associated with the surface membranes at 4°C either singly or in groups of 2-4, and were localized predominantly to the outer most extensions of the folds. The association of the gold particles with the cell surface was not uniform over the entire cell circumference, but displayed a distinct polarity. The positioning of the Golgi elements and the microtubule organizing centers (MTOC) over one pole of the nucleus defined a cell axis along which extensive microtubule (MT) arrays ran perpendicular to the cell surface; the majority of the gold particles were localized on the cell surface directly above these MT arrays.

No gold particles were observed along the surface of cells incubated with Au_{16}-BSA or with 16 ug Au_{16}-hCG in the presence of 100 ug unbound hCG (Fig. 9). Single gold particles were occasionally observed along the plasma membrane of the cells treated with Au_{16}-BSA after 90 min., but these gold particles were never observed inside the cell.

After the Au_{16}-hCG labeled cells were warmed to 37°C for 15-30 min., gold particles were clustered on the folds of the cell surface (Fig. 10), and concentrated in the coated pit regions at the base of the folds (Fig. 11,12). 60 min. after warming, Au_{16}-hCG was concentrated in smooth surfaced vesicles that were designated as initial endosomes (Endosomes I), and in lysosome-like structures near the cell surface (Fig. 13). The initial endosomes were

Figure 7: Diffuse Binding of Au_{16}-hCG to Luteal Cell Surfaces at 4°C.

Diffuse binding of Au_{16}-hCG to microvilli along the surface of a luteal cell incubated with Au_{16}-hCG for 4 hours at 4°C. Arrows indicate gold beads associated with microvillar membrane (X20,000).

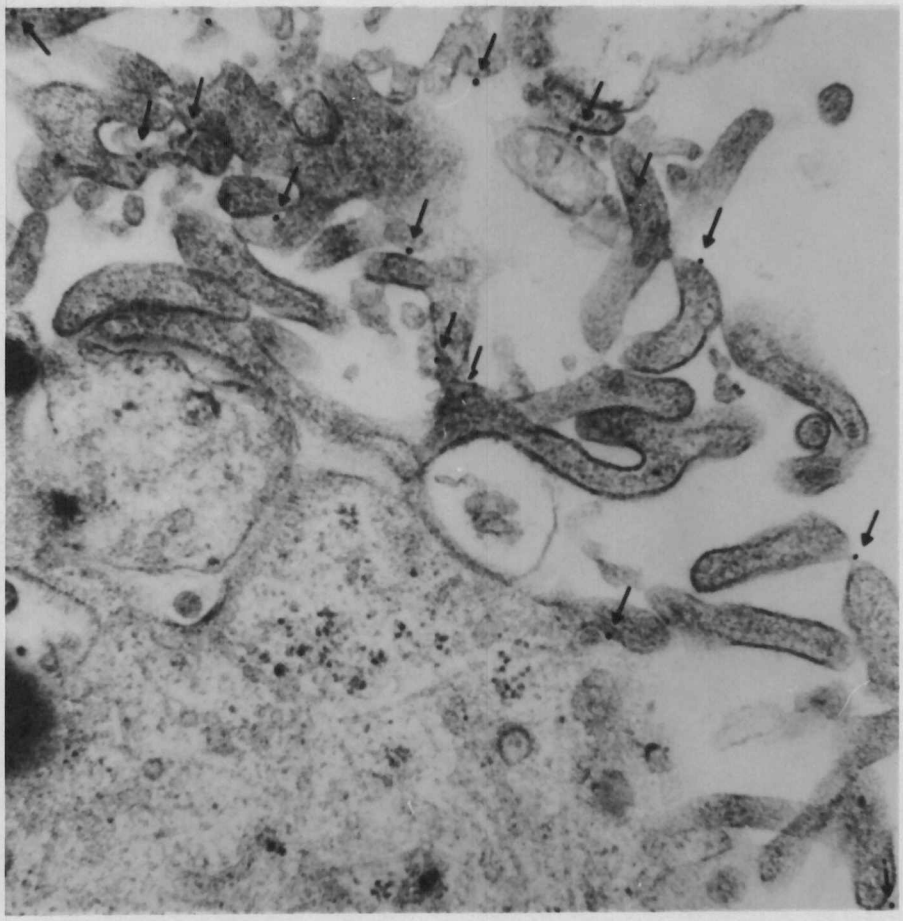
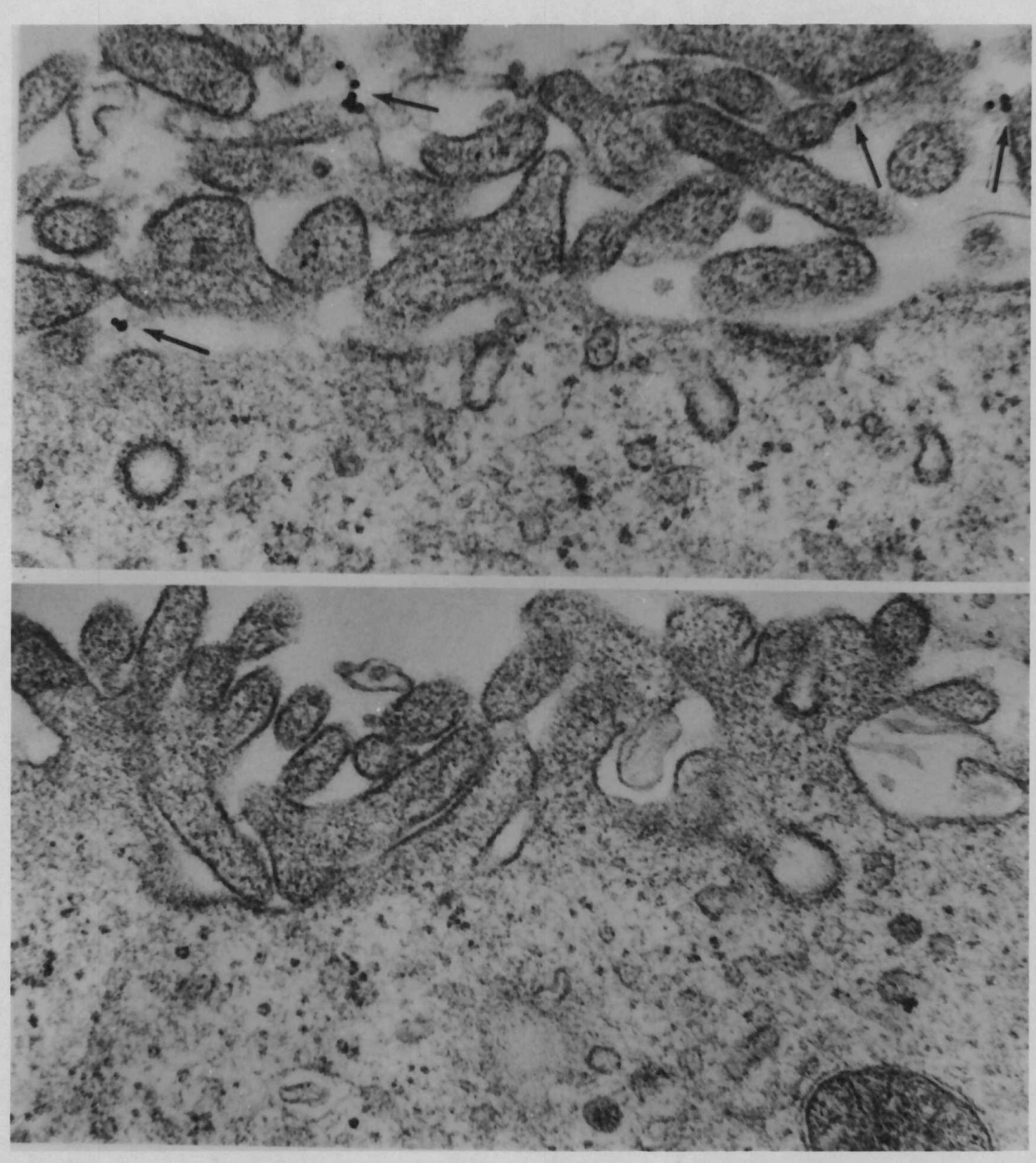


Figure 7

Figure 8: Binding of Au_{16}-hCG to Luteal Cell Surfaces at 4°C. Electron micrograph of a luteal cell incubated with Au_{16}-hCG for 4 hours at 4°C that demonstrates binding of Au_{16}-hCG to microvilli and folds along the cell surface. Arrows indicate gold beads associated with the cell surface membrane (X60,000).

Figure 9: Binding of Au_{16}-hCG to Luteal Cell Surfaces with Excess hCG. Electron micrograph of the surface microvilli of a luteal cell incubated with Au_{16}-hCG in the presence of excess native hCG for 4 hours at 4°C. No gold beads were observed to associate with cell surface membrane (X50,000).



Figures 8 and 9

Figure 10: Binding of Au_{16}-hCG to Luteal Cell Suspensions at 37°C after 30 min. Cluster of Au_{16}-hCG bound to the microvilli of a luteal cell incubated with Au_{16}-hCG for 4 hours at 4°C, and warmed to 37°C for 30 min (X96,000).

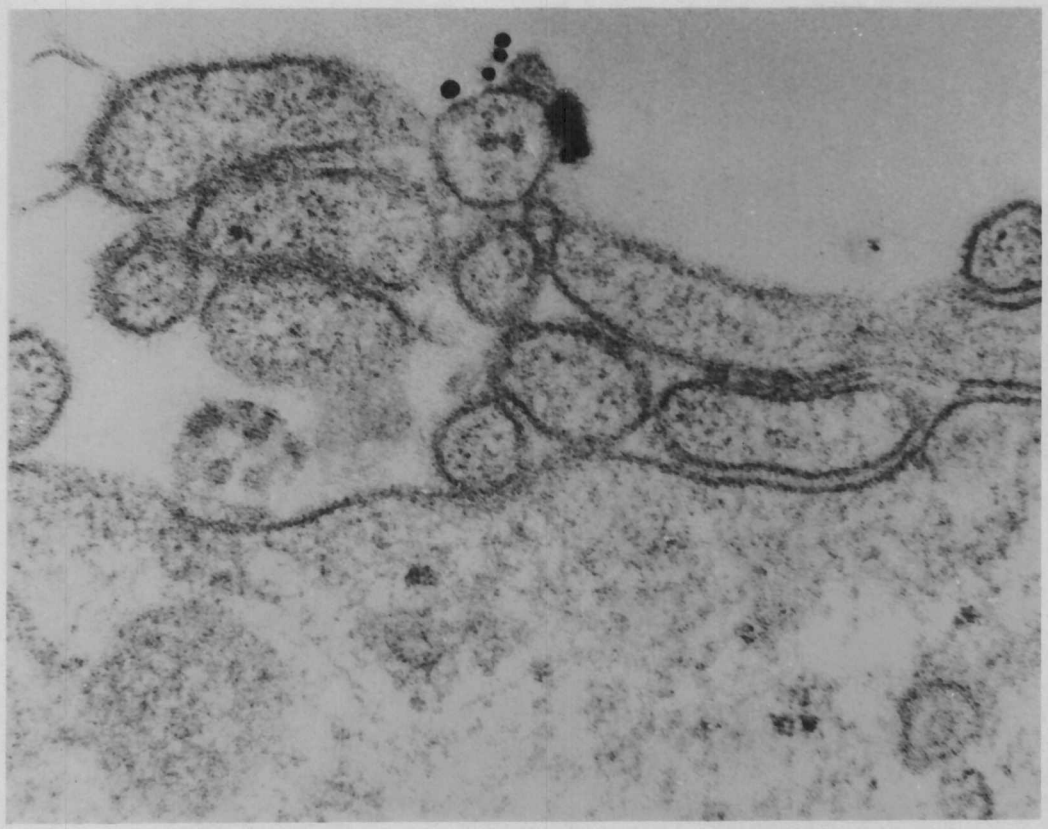


Figure 10

Figure 11: Binding of Au_{16}-hCG to Luteal Cell Surfaces at 37°C after 60 min. Cluster of Au_{16}-hCG adjacent to a coated pit on the surface of a luteal cell incubated with Au_{16}-hCG at 37°C for 30 min. Arrows indicate gold beads associated with microvillar extensions (X65,000).

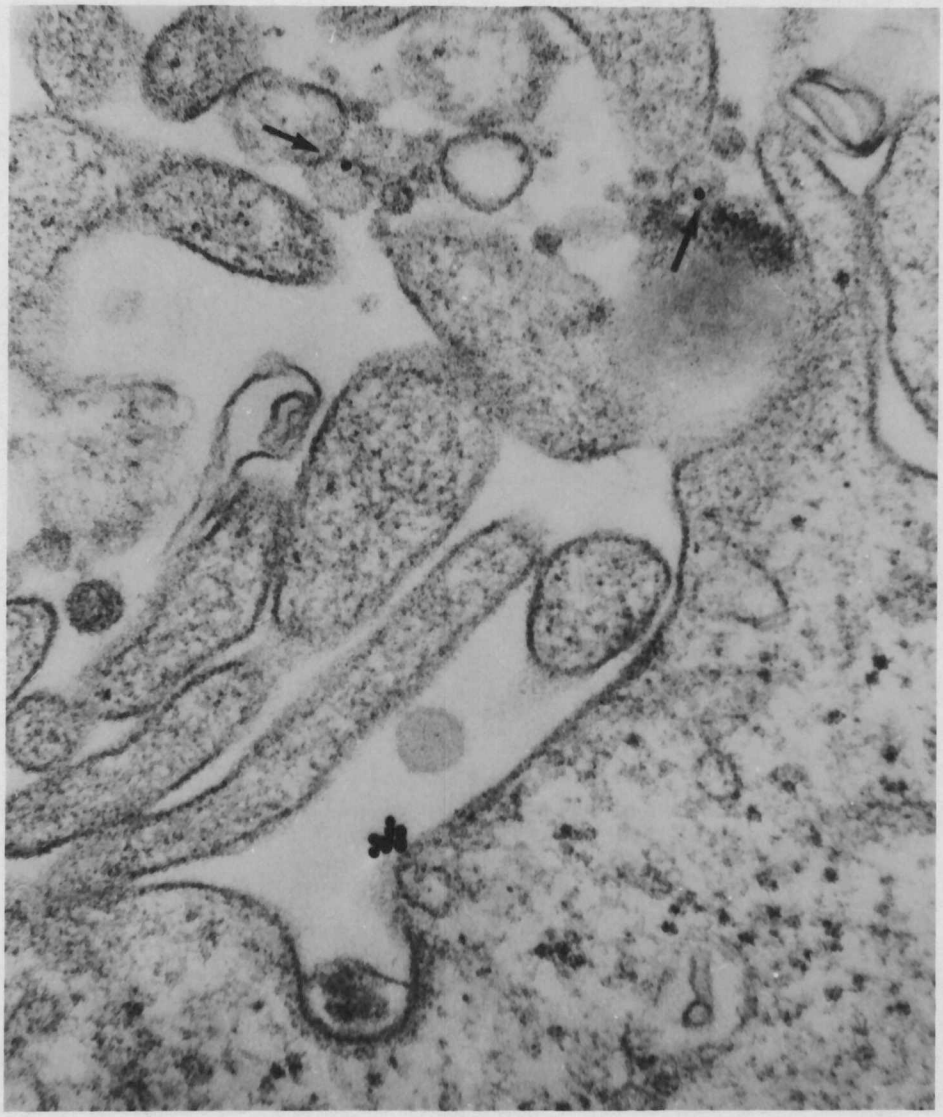


Figure 11

Figure 12: Internalization of Au_{16}-hCG in Coated Pits. Coated vesicle labeled with Au_{16}-hCG on the surface of a luteal cell incubated with Au_{16}-hCG for 30 min. at 37°C (X124,000).

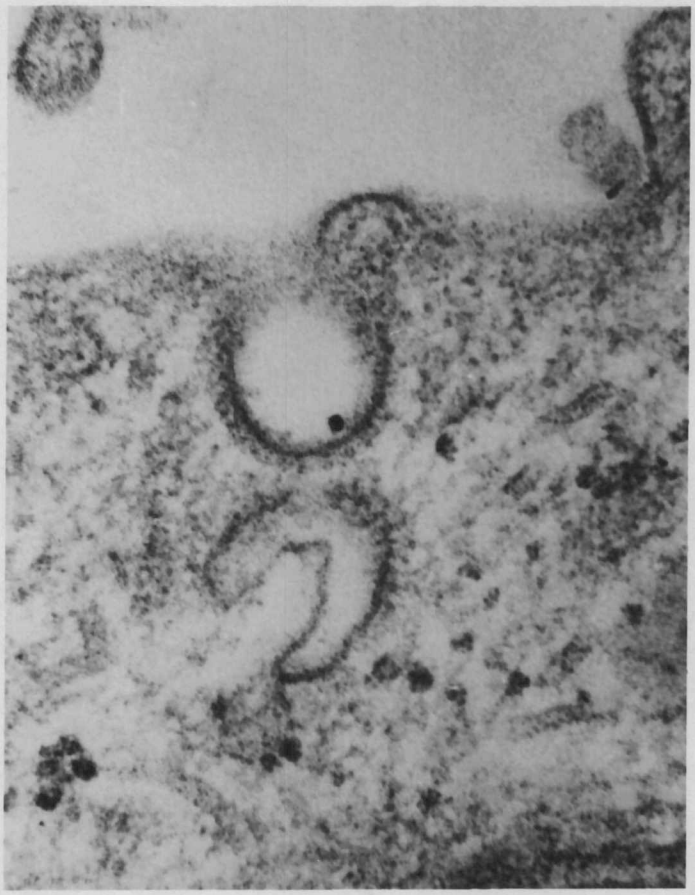


Figure 12

Figure 13: Internalization of Au_{16}-hCG in Initial Endosomes. Initial endosome labeled with Au_{16}-hCG that occupies the peripheral regions of a luteal cell incubated with Au_{16}-hCG for 60 min. at 37°C. Note ruffle forming along the plasma membrane of the luteal cell. Arrow indicates Au_{16}-hCG associated with the luteal cell surface (X50,000).



Figure 13

approximately 600-800 nm in diameter, and were characterized by dense plaques with associated filamentous structures on the wall of the vesicle that were directly adjacent to gold particles. The heterogeneous contents of the initial endosomes were usually displaced to the perimeter, leaving a clear central area possessing fine filamentous networks (Fig. 14). In contrast, the gold particles in the lysosome-like structures were distributed among closely packed vesicular contents of heterogenous electron density (Fig. 15).

After 90 min. another distinct class of smooth surfaces vesicles containing gold particles were observed in the centrospheric region of the cell, and proximal to MTOC, and the perimeter of the golgi elements. This class of structures was designated as secondary endosomes or endosomes II (Fig. 16,17). At no time were large number of gold particles present in the secondary endosomes. For example, an average of 2.2 or 1.5 gold particles were observed inside endosomes occupying the MTOC and Golgi regions respectively as compared to 6-100 gold particles observed inside initial endosomes or the lysosome-like structures occupying the apical cell regions.

Two distinct classes of secondary endosomes were observed according to the morphology of the vesicle contents. Gold labeled secondary endosomes either contained closely packed heterogenous elements of high electron density, or were filled with a lacy filamentous element. The diameter of secondary endosomes was correlated according to cellular locale. The average diameter of gold containing endosomes adjacent to the Golgi apparatus ranged from 250-800 nm, in contrast to gold containing endosomes occupying MTOC regions that appeared in two subgroups with diameters of 800-1000 nm or 300 nm. However, the characteristics of the contents of the secondary endosomes were not correlated with the endosome locale of Golgi or MTOC regions.

Figure 14: High Magnification of Initial Endosome. High magnification of initial endosome from Figure 13. A dense plague with associated filamentous structures is observed along the cytoplasmic face of the limiting membrane that is directly adjacent to gold beads (X100,000).

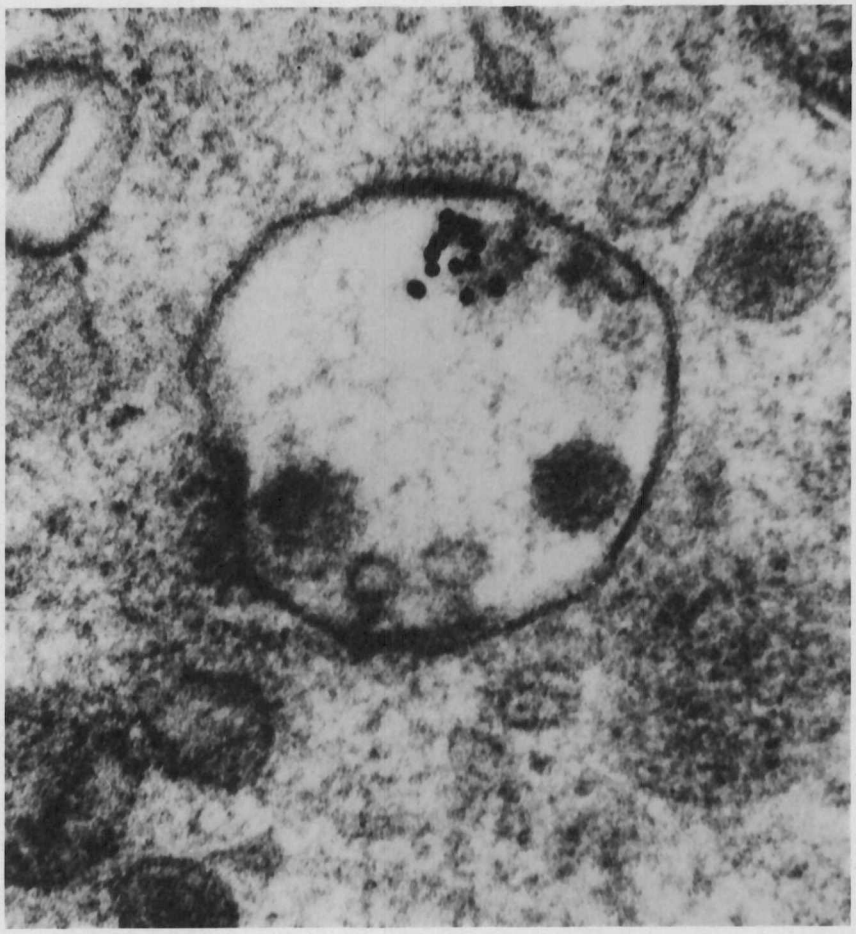


Figure 14

Figure 15: Localization of Au_{16}-hCG in Multivesicular Bodies. Au_{16}-hCG (arrows) localized in a multivesicular body (mvb) positioned directly beneath the cell surface (cs) of a luteal cell incubated with Au_{16}-hCG for 60 min. at 37°C. Arrows also indicate gold beads associated with the cell surface membrane (X80,000).

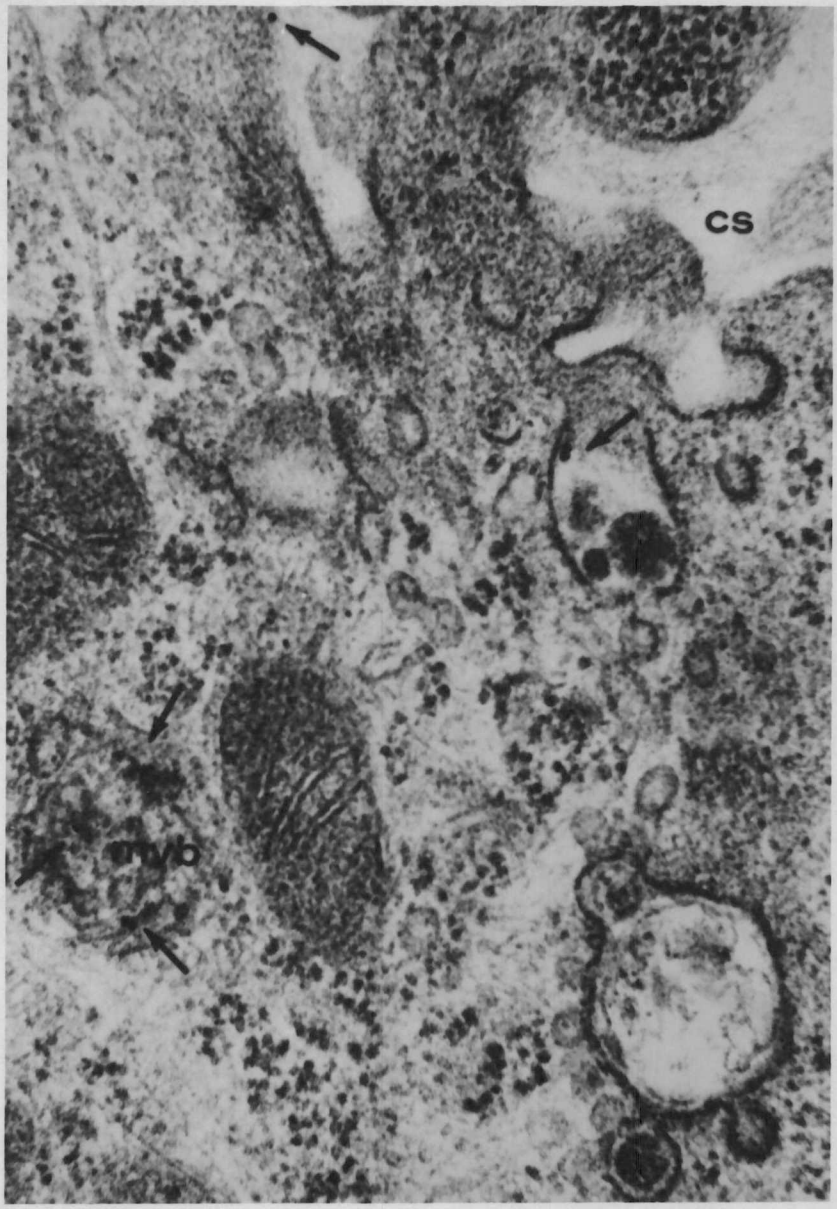


Figure 15

Figure 16: Au_{16}-hCG in MTOC Associated Secondary Endosomes. Secondary endosomes labeled with Au_{16}-hCG (arrows) that are positioned in the centrosphere of luteal cells incubated with Au_{16}-hCG for 90 min. This grouping of secondary endosomes are directly adjacent to a cytoplasmic thickening that appears to be a microtubule organizing center (mtoc) (X39,000).

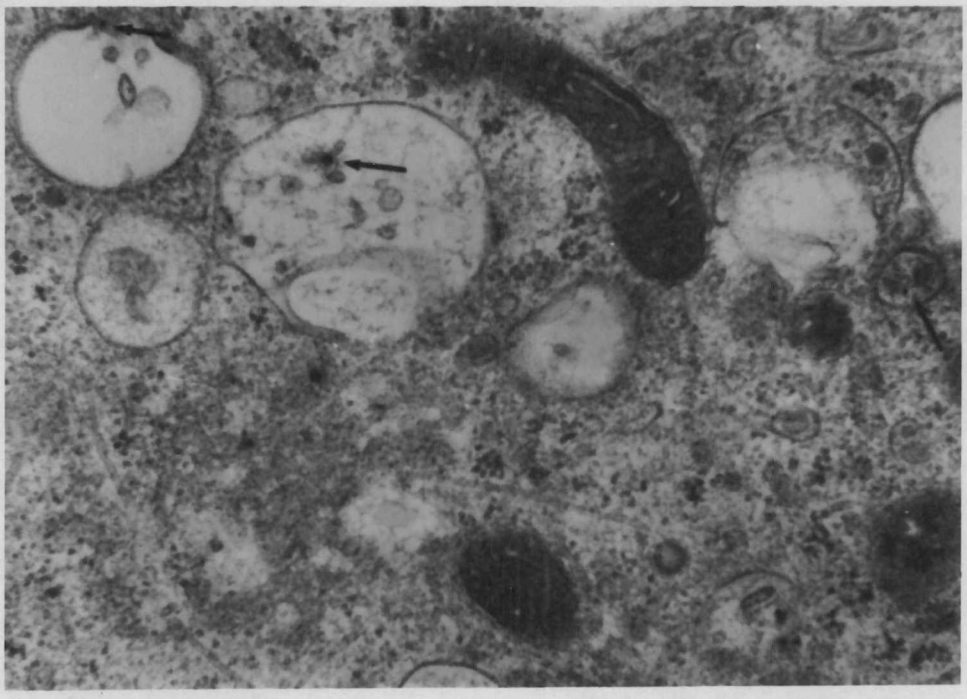


Figure 16

Figure 17: Au_{16}-hCG in Golgi Associated Secondary Endosomes. Secondary endosomes labeled with Au_{16}-hCG (arrows) that are positioned directly adjacent to a Golgi apparatus (G) (X45,000).



Figure 17

2. Cells Incubated with Au_{16}-hCG at 4°C only

In some experiments, cells were incubated with 20 ug Au_{16}-hCG for 4 hrs. at 4°C, rinsed and resuspended in media, and warmed to 37°C for 15, 30, 60 and 90 min. The pathway of internalization of gold particles appeared to be identical to the pathway observed in cells treated with Au_{16}-hCG throughout all incubation at 37°C: coated vesicles to smooth surfaced initial endosomes or lysosome-like structures followed by translocation to centrospheric regions. In the first set of experiments (1), gold particles were localized along the cell surface at all time points through 90 min. at 37°C when Au_{16} hCG was administered as a pulse at 4°C and the cells then warmed up to 37°C. In these experiments, all gold particles appeared to have cleared from the cell surface after 30 min. The total number of gold particles observed inside these cells was also markedly reduced over 90 min. at 37°, compared to the cells exposed to Au_{16}-hCG through 90 min at 37°C.

In all experiments, a higher number of gold particles were associated with the cell surfaces of small luteal cells than were observed on the surface of large luteal cells. The endocytic pathway employed by both large and small luteal cells during the internalization of Au_{16}-hCG appeared to be identical.

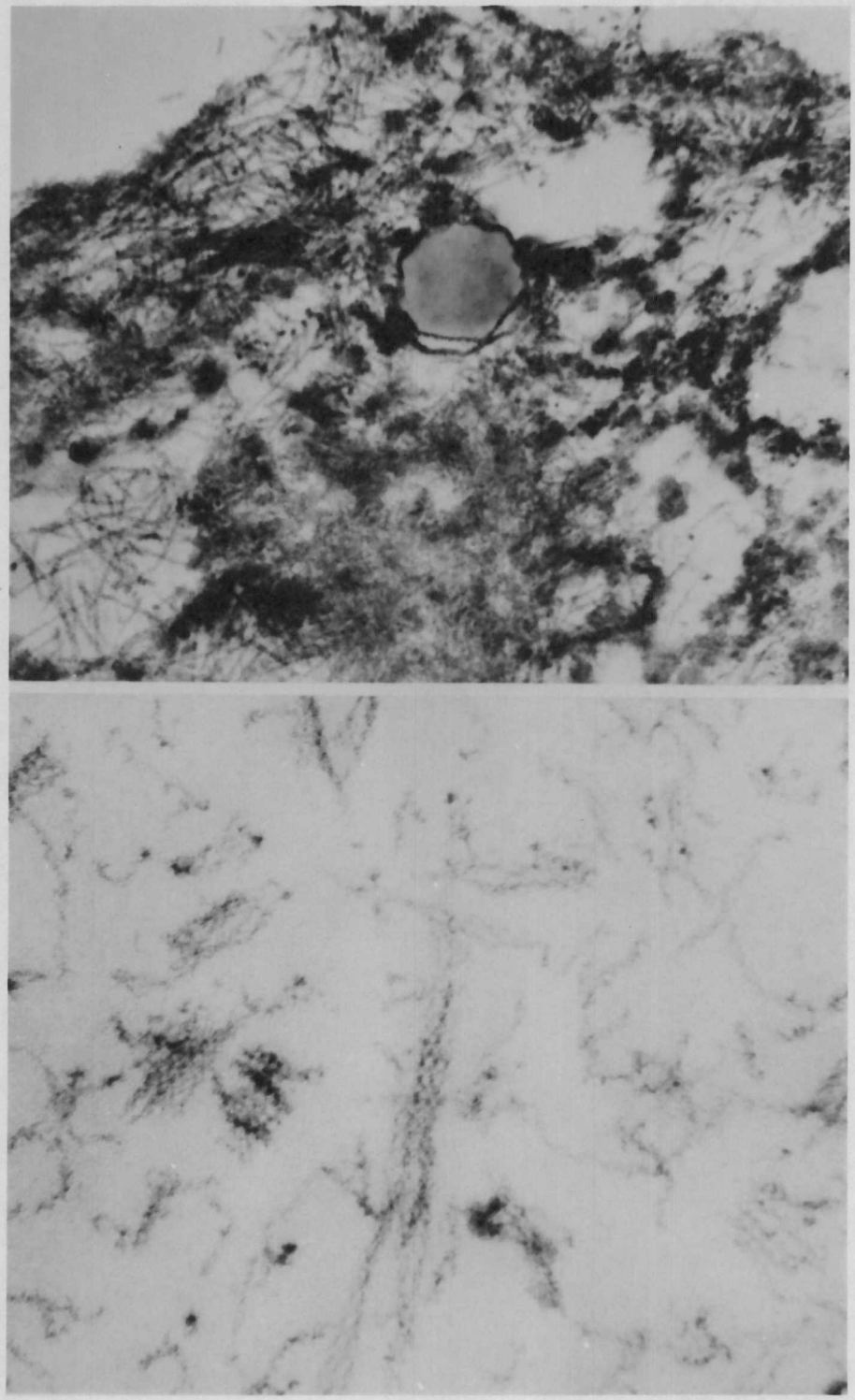
C. The Cytoskeleton of Luteal Cells

1. Microfilaments in Thin Section

In the experiments where luteal cell suspensions were treated with ethanol and incubated with myosin S-1, decorated filaments exhibiting the characteristic arrowhead configuration and a detectible polarity were abundant throughout the cytoplasm (Fig. 18,19). The complex interconnecting networks of decorated

Figure 18: S-1 Decorated Microfilaments in Luteal Cells. Luteal cell that has been permeated with ethanol and incubated with myosin subfragment-1. Numerous decorated microfilaments are observed directly beneath cell surface membrane and throughout the cytoplasm (X27,500).

Figure 19: High Magnification of S-1 Decorated Microfilaments. High magnification of microfilaments decorated with myosin S-1 that were localized in the cytoplasm of luteal cells treated with ethanol. Note the arrowhead configurations (X80,000).



Figures 18 and 19

filaments were most apparent in regions adjacent to the cell surface membrane. Here, decorated filaments extended from regions of the plasma membrane that were dense with adherent cytoplasmic materials, and interacted with other decorated filaments, or terminated on the surface of various subcellular structures. Decorated filaments were also observed in centrospheric regions, particularly concentrated in areas previously occupied by lipid droplets, lysosomes, or whorls of smooth endoplasmic reticulum (Fig. 19).

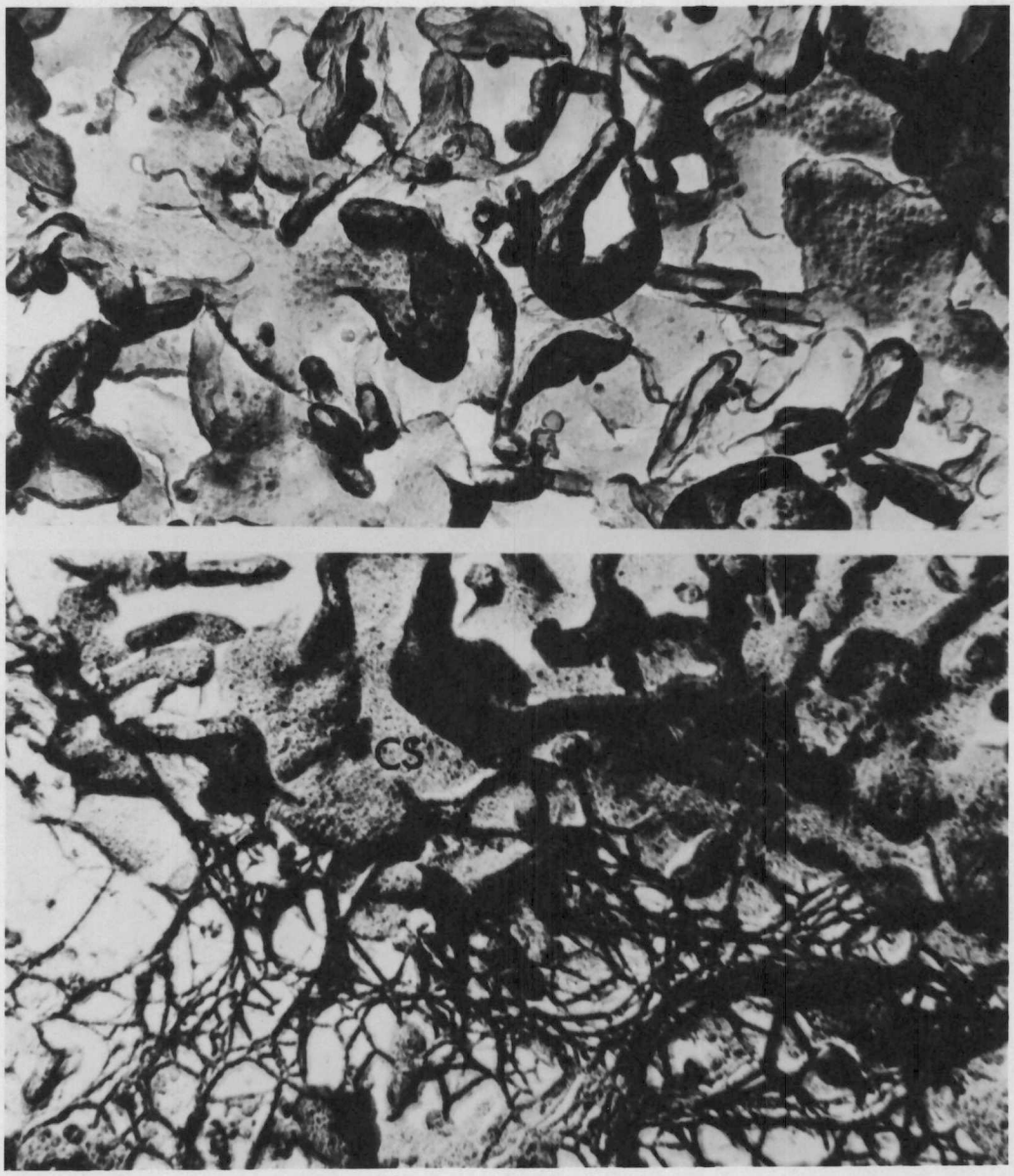
2. Replicas

Luteal cells that had been cracked open and incubated with myosin S-1 in the presence of proteolytic inhibitors, were critical point dried, and replicated with platinum/carbon. Examination of three dimensional images form the replicas provided a unique perspective into the complex interconnections that characterize cytoskeletal organization. However, the quality of the replica varied widely within a single grid. One area would be almost transparent having received little metal coating, while an adjacent area would be coarsely defined by heavier metal depositions. Accordingly, measurements of filament diameter varied widely with the quality of the metal coating in a particular region of the grid.

The observed interaction of filamentous structures from various classes of cytoskeletal elements, as well as the spacial arrangement of subcellular organelles by the cytoskeletal elements differed widely between subcellular locale. For example, a replica of an area near the plasma membrane of a cracked cell revealed an anastamosing array of filaments that bridged the space between the surface membrane and the underlying cytoplasm (Fig. 20,21). The plasma membrane in this replica was characterized by folds and microvilli

Figure 20: Replica of Luteal Cell Surface. Platinum and carbon replica of the surface of a luteal cell exhibiting numerous microvilli and cytoplasmic folds or extensions (X30,000).

Figure 21: Replica of Luteal Cell Surface that was Cracked. Platinum and carbon replica of the peripheral regions of a luteal cell that has been cracked open. A region of the cell surface membrane (cs) occupies to top right portion of the electron micrograph. A grouping of cytoskeletal elements directly connects to this surface membrane, and also connects with underlying subcellular organelles (bottom left) (X24,000).



Figures 20 and 21

with a granular surface that was identical to the topography observed on the surface membranes of cells that had not been cracked (Fig. 20).

3. The Cytoskeleton and the Endocytic Pathway

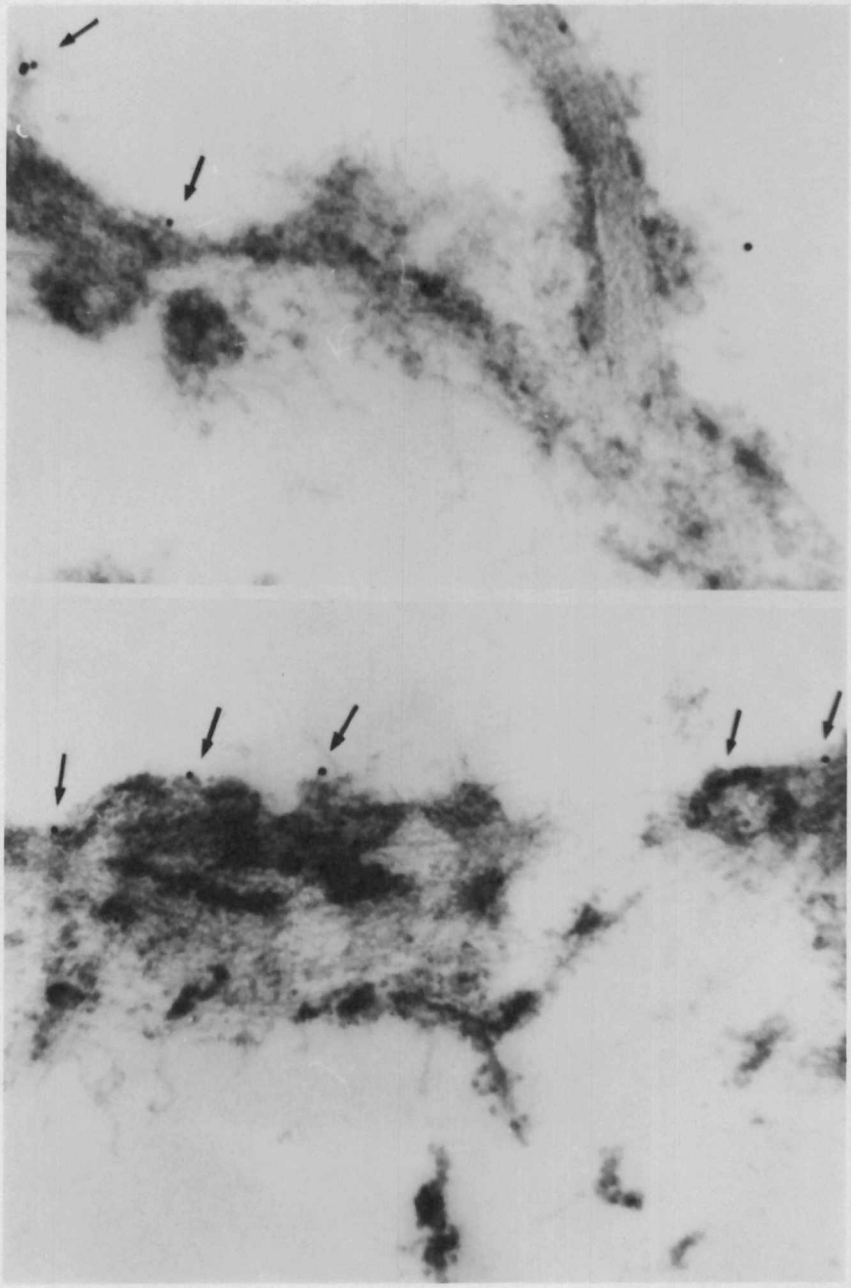
Some luteal cells were incubated with Au_{16}-hCG, and subsequently with myosin S-1 in order to perform double labeling experiments. The plasma membranes in these preparations were thick and highly electron dense with cytoplasmic materials adhering to the inner surface. Decorated filaments were present and were observed to connect directly to the cytoplasmic surface of the plasma membrane. They were repeatedly observed to be abundant at sites where gold particles were localized to the exterior of the surface (Fig. 22,23). Decorated filaments were not observed to directly associate with coated cavealae.

Membrane bound vesicles containing gold particles in the centrospheric regions of the cell were present in cells treated with ethanol alone, but not cells treated with ethanol and incubated in myosin S-1.

Intermediate filaments were observed in close apposition to all subcellular structures labeled with gold particles. Filaments of 10 nm in diameter appeared to be associated directly with a coated vesicle containing Au_{16}-hCG that was located directly beneath the plasma membrane (Fig. 24,25). Arrays of intermediate filaments were also readily apparent in cells that were incubated with Au_{16}-hCG and treated with ethanol without subsequent incubation with myosin S-1. Loose bundles of intermediate filaments that were associated directly with lysosome-like structures filled with gold particles were also inserted into the outer membrane of the nuclear envelope (Fig. 26).

Figure 22: S-1 Decorated Microfilaments in Au_{16}-hCG Treated Cells. Portion of the surface of a luteal cell that was incubated with Au_{16}-hCG for 60 min. at 37°C, permeated with ethanol, and incubated with myosin subfragment-1. Arrows indicate gold beads associated with the cell surface. Note decorated microfilaments with discernable polarity in the interior of the microvilli (X48,000).

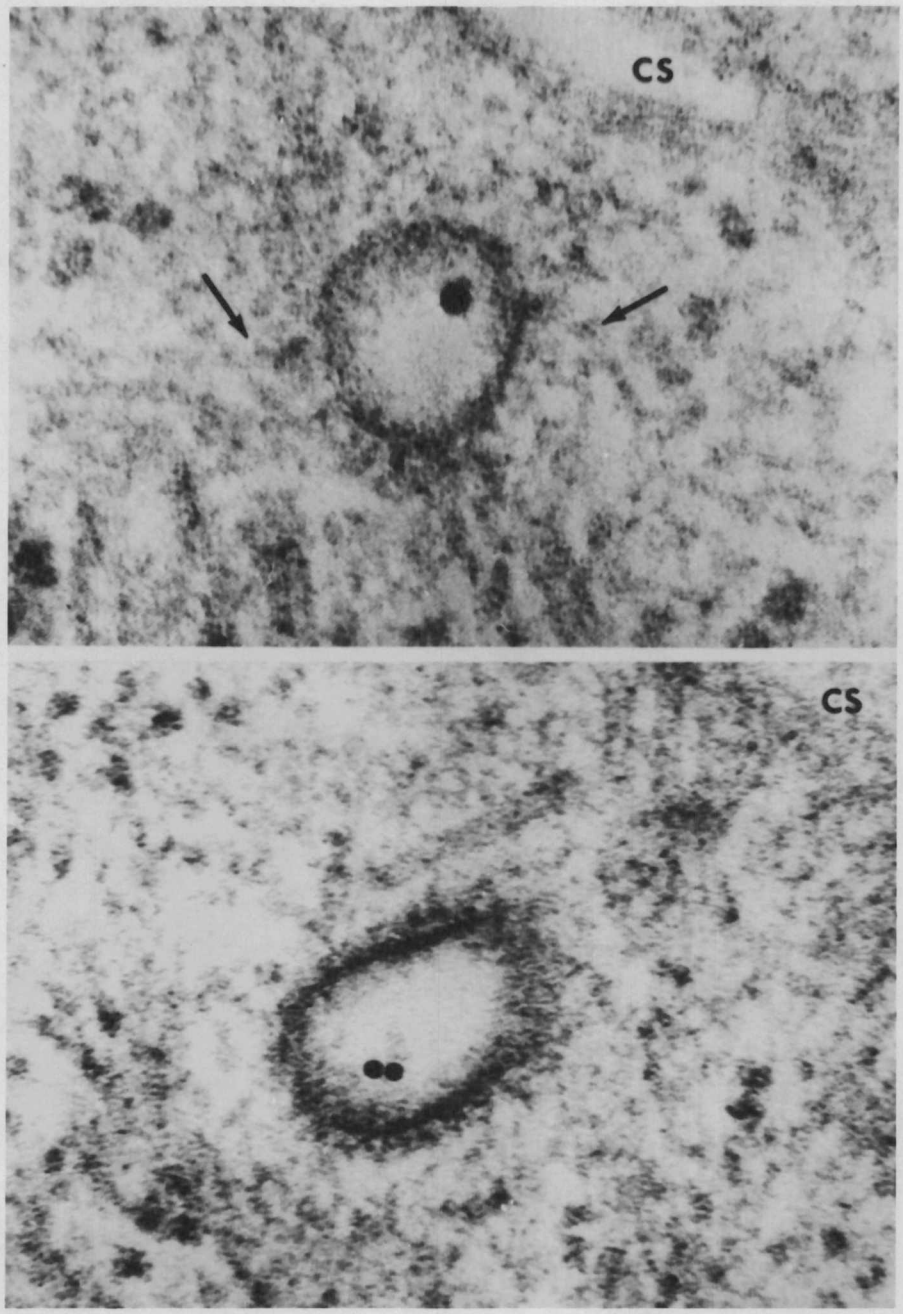
Figure 23: S-1 Decorated Microfilaments in Au_{16}-hCG Treated Cells. Portion of the surface of a luteal cell that was incubated with Au_{16}-hCG for 60 min. at 37°C, permeated with ethanol, and incubated with myosin subfragment-1. Arrows indicate gold beads associated with the cell surface (X40,000).



Figures 22 and 23

Figure 24: Intermediate Filaments and Au_{16}-hCG Labeled Coated Vesicle. Coated vesicle labeled with Au_{16}-hCG that is located near the surface of a luteal cell (cs). Arrows indicate filaments that are 10 nm in diameter that appear to insert directly into the coated vesicle (X226,000).

Figure 25: Microtubules and Au_{16}-hCG Labeled Coated Vesicles. Coated vesicle labeled with Au_{16}-hCG that is located near the surface of a luteal cell (cs). Note microtubule oriented in parallel with the long axis of the coated vesicle (X132,000).



Figures 24 and 25

Figure 26: Intermediate Filaments and Au_{16}-hCG Labeled Lysosomes. Electron micrograph of a luteal cell incubated with Au_{16}-hCG for 60 min. at 37°C, and permeated with ethanol. Arrows indicate a grouping of gold beads with a lysosome like structure. Intermediate filaments (IF) are positioned between the gold labeled structures and the cell nucleus (X43,000).

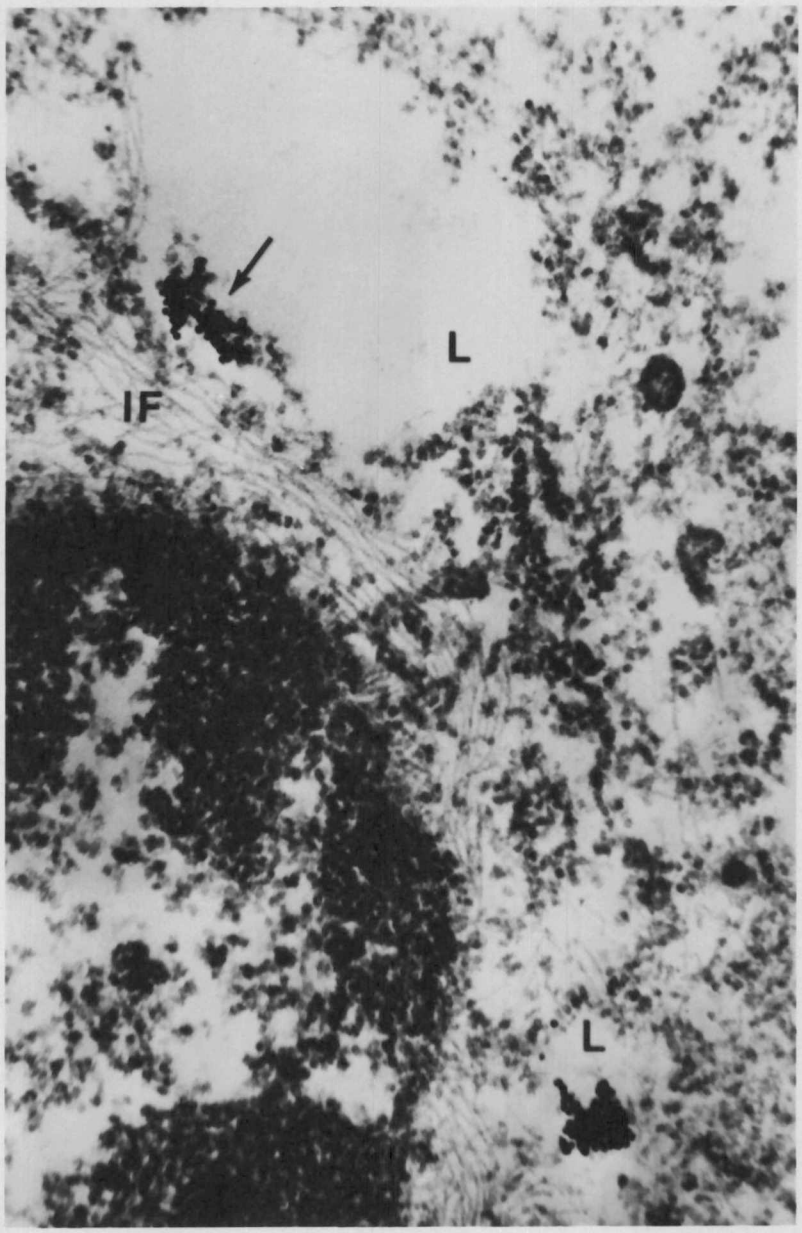


Figure 26

Microtubules (MT) were numerous in cell regions that were active in endocytosis, and were observed along the long axis of a gold-labeled coated vesicles (Fig. 25). Microtubules were also abundant in the Golgi and MTOC regions and were interspersed between secondary endosomes containing gold particles (Fig. 16,17).

CHAPTER IV

DISCUSSION

A. Receptor-mediated Endocytosis of Au_{16}-hCG

This study produced evidence that human chorionic gonadotropin can be internalized by fully differentiated porcine luteal cells maintained in suspension cultures. Three lines of evidence indicated that Au_{16}-hCG was internalized by a receptor-mediated mechanism:

1. Binding took place on microvillar processes along luteal cell surfaces at 4°C. Internalization was not observed until cells were warmed to 37°C. This observation was consistent with the temperature dependent inhibition of receptor-mediated endocytosis of insulin, EGF, $_2$M, and hCG by fibroblastic and granulosa cells respectively (91,93,102,103,138,139,140,115,46,30,31,1,87). The exact mechanism by which reduced temperature operated to inhibit receptor-mediated endocytosis has not been elucidated. However, a reduction in the production of ATP was correlated with temperature-induced blockage of fluid phase pinocytosis in 3T3 cells (123,124). In this study, intracellular ATP levels were lowered by reducing temperature (i.e. reducing the likelihood of glycolytic enzymes obtaining sufficient activation energy). Steinman also suggested that reduced production of ATP resulted in the inhibition of pinocytosis by modifying the viscosity of surface membrane lipids or by altering the organization of cytoskeletal elements that normally participate in the endocytic event (123,124). Temperature dependent inhibition of internalization in luteal cells is probably also controlled by one or more of these mechanisms. The temperature sensitivity of internalization did, however, provide evidence

that were consistent with the concept that the binding of Au_{16}-hCG was receptor-mediated.

2. Two observations indicated that the binding of Au_{16}-hCG to luteal cell surfaces at 4° or at 37°C was specific: a. the addition of an excess of unlabeled hCG during incubation at 4°C or at 37°C effectively competed for Au_{16}-hCG binding sites along the surface of luteal cells. b. A conjugate of Au_{16}-BSA was prepared in order to determine whether a gold conjugate of any type could non-specifically absorb onto luteal surface membranes. Luteal cells did not bind Au_{16}-BSA at 4°C, and only minimally after 1.5 hours.

Since native hCG effectively competed with Au_{16}-hCG for binding sites along the cell surface, and Au_{16}-hCG did not appear to associate with surface membranes due to the charge of the gold complex alone, the binding of Au_{16}-hCG to luteal cell membranes was interpreted to be specific. Specificity of binding is also a criterion for a receptor-mediated event (Silverman et al., Steinman et al.).

3. A third line of evidence also indicated that the association of Au_{16}-hCG to luteal cell surfaces was probably receptor-mediated. Luteal cells responded to incubation with Au_{16}-hCG by releasing increased amounts of progesterone into the incubation media. Cells incubated with Au_{16}-BSA responded with basal progesterone release alone. These results are in agreement with previous reports that ^{125}I-hCG and native hCG stimulated luteal cells to release comparable amounts of progesterone (62,29,82,114,119). The Au_{16}-hCG induced progesterone release by luteal cells observed in this study was interpreted to be a result of the binding of Au_{16}-hCG (cells incubated at 4°C only released minimal progesterone). Furthermore, the inducement of a

physiological response from cells incubated with Au_{16}-hCG is consistent with the notion that the binding of Au_{16}-hCG to luteal cell surfaces is indeed receptor-mediated (118,123).

B. Corroboration of Earlier Reports

The observation that Au_{16}-hCG binds diffusely to microvillar processes of porcine luteal cells in vitro at 4°C, and becomes internalized by coated regions of surface membrane at 37°C, corroborates several earlier reports (87,30,31,5,6,36). In these studies, luteal cells in vitro and in vivo, as well as cultured granulosa cells, were observed sequentially to: 1) bind ^{125}I-hCG to microvillar processes along pericapillary spaces, 2) internalize the ^{125}I-hCG-receptor complex (36) in coated vesicles (30,31,1), and 3) concentrate the labeled hormone in multivesicular bodies (5,6,36,1,30,31), where it was degraded to its constituent amino acids (30,31). These studies indicated that hormone was localized intracellularly between 3-7 hours following the original administration. Our study provides evidence that luteal cells in vitro initiate the internalization of surface associated Au_{16}-hCG by 10 min. at 37°C, and that binding and internalization continue up to 2 hours. These observations substantiate an earlier report that describes the internalization of LH-ferritin by rat luteal cells (87). Suspensions of rat luteal cells were observed to internalize ferritin-LH within minutes following administration of hormone at 37°C. Ferritin-LH was endocytosed in coated vesicles, and later observed in lysosomal-like structures. The data presented here, when considered with the data previously reported suggest that the internalization of LH and hCG by isolated luteal cells in vitro occurs more rapidly then in luteal cells in vivo but by similar mechanisms.

C. Polarity of Binding

Au_{16}-hCG was not observed to bind uniformly over the porcine luteal cell surface as previously reported in luteal cells that were prepared by enzymatic dissociation (87). Rather, surface binding displayed a distinct polarity. Binding occurred preferentially along a microvillus border that was defined by the position of microtubular arrays originating from over one pole of the nucleus. This pattern of binding appears to be analogous to earlier reports that ^{125}I-hCG bound preferentially to the cell surface microvilli that were directly adjacent to the pericapillary space (1,30,31). The presence of gap junctional complexes at the apical cell regions between luteal cells in vivo was documented, and was suggested to impede the accessibility of ^{125}I-hCG to any receptors that were located at the basolateral cell surfaces (10). Gap junctions were not observed along the plasma membranes of the porcine luteal cells employed in this study, and were assumed to be internalized or destroyed as a result of the dissociation procedure. However, we observed repeatedly that binding of Au_{16}-hCG was polarized, and that this polarity was maintained in cells that were dissociated and incubated in suspension for several hours.

D. Initial Endosomes Compared to Receptosomes

Following incubation for 30 min. at 37°C, Au_{16}-hCG began to accumulate in coated regions of the luteal cell surface membranes that were located predominantly at the bases of microvillar extensions. Au_{16}-hCG that was observed to be internalized in coated vesicles and to also appear in a series of smooth surfaced vesicles that were termed initial endosomes. The initial endosomes observed in fully differentiated luteal cells employed in this study bear striking resemblance to the receptosomes observed in a variety of cultured

cell lines (102,103,138,139,140), and to the tubulovesicular structures observed in hepatocytes (130). The data presented in this study, when taken with data from a variety of other cell systems (130,102,103,138,139,140,91,92,93,129,123) supports the hypothesis that ligand internalized by a receptor-mediated mechanism passes through a series of smooth surfaced vesicles prior to delivery to other subcellular locale. These data extend this hypothesis by showing that this process is applicable to at least one large highly differentiated parenchymal cell as well as the cultured cell lines used to elucidate the process.

E. Content of Initial Endosomes

Much attention is now being directed at understanding the fate of the hormone-receptor complex following its entrance into the series of smooth surfaced vesicles. Willingham and Pastan advanced the hypothesis that the receptosome represented the subcellular locale from which receptors were recycled to the cell surface, and from which ligand was shuttled to the GERL (98) prior to delivery to lysosomes (92,102,103,138,139,140). Although a variety of ligands have been observed inside receptosomes, only one receptor, the phosphomannosyl receptor, has been localized to the interior of receptosomes (139). No attempt was made during the present study to determine if the initial endosomes that contained the labeled gold particles, presumably Au_{16}-hCG, also contained the hCG receptors. In fact, the following observations lent support to the notion that Au_{16} observed in initial endosomes probably did not remain attached to the receptor molecule:

a) The majority of Au_{16}-hCG observed in initial endosomes did not appear to be membrane bound. This could be a result of the thin sectioning technique and a physical pushing away from the membrane, an oblique section

which did not reveal the proximity of the membrane, the failure of the observed gold particle and the ligand on it to form a hormone receptor complex in the first place, or ligand uncoupled from its receptor. This latter point was consistent with a recent observation by Zimmiski et al., (142,143). They observed that most ^{125}I-hCG was not only free from its receptor following internalization, but also retained the ability to rebind the LH receptor in a Leydig tumor cell bioassay once re-isolated.

b) Initial endosomes that were labeled with Au_{16}-hCG in luteal cells bore striking resemblance to the body of CURL (Compartment of Uncoupling of Ligand and Receptor), that was prominent during period of active internalization of asialoglycoproteins by hepatocytes in vivo (49,130). In hepatocytes the tubular extensions that were in communication with the main body of CURL actively sequestered asialoglycoprotein receptors that were uncoupled from the asialoglycoproteins. The asialoglycoproteins remained free in the lumen of CURL. The body of CURL in time gained morphological characteristics of a secondary lysosome. In addition, it was suggested that a drop in pH inside the lumen of CURL represents a prerequisite for the activation of a series of hydrolytic enzymes.

We did not attempt to determine whether the initial endosomes containing the presumptive Au_{16}-hCG represented a subcellular compartment characterized by an intralumenal low pH. However, the similarities between the morphology of the initial endosomes in luteal cells, and the body of CURL in hepatocytes suggest that this may very well be the site where dissociation of hCG from its receptor takes place in the luteal cell.

F. Secondary Endosomes

We presented evidence for the first time that hormone internalized by cultured luteal cells appeared in a series of smooth surfaced vesicles deep within the cell centrosphere, and termed these vesicles secondary endosomes. The majority of these vesicles labeled with the gold marker were in close apposition to transverse Golgi elements which probably represented a portion of the GERL. Although the Golgi apparatus has been thought to be active in the processing of ligands and receptors during receptor-mediated endocytosis in a variety of cells (7,8,9,51,52,102,103,138,139,140,53,54), the role of the Golgi during the receptor-mediated endocytosis of hCG by luteal cells has remained unclear. We were unable to determine whether the receptor accompanied the hormone to the secondary endosome. In addition the possibility existed that the hCG molecules were rapidly detached from the gold bead following endocytosis. Since endosomes in other cell types have been demonstrated to exhibit a drop in pH during internalization there is a strong possibility that this also occurs in luteal cells (129). Solutions of Au_{16} were observed to be destabilized at pH 3-4.5, and formation of Au_{16}-hCG was not successful at a pH below 4.5. Therefore there is a strong possibility that the ligand and gold particle could be separated shortly after internalization took place.

G. Cytoskeletal Elements and the Internalization of Au_{16}-hCG

Cytoskeletal elements were repeatedly observed in positions directly adjacent to all of the different membranous components labeled with or enclosing Au_{16}-hCG. In addition, intermediate filaments and S-1 labeled microfilaments appeared to be linked structurally to regions of the plasma

membrane occupied by the presumptive Au_{16}-hCG-receptor complexes (Figures 12-15, 19-21). These findings were consistent with earlier reports describing the reorganization of cytoskeletal elements concommitant with the internalization of hormone:

Batten et al. (14) observed that the predominant species of cytoskeletal elements in cultured granulosa cells were microfilaments, and that their arrangements included a subplasmalemal network, and cell-wide stress fibers. These stress fibers were observed to depolymerize accompanying the onset of receptor-mediated endocytosis of FSH. Albertini and his colleagues (4,3,64,65) examined the role of microtubules and intermediate filaments during the RME of FSH by granulosa cells. Specifically, MT and IF were implicated in the movement of surface associated endosomes to the centrosphere of granulosa cells. Using indirect immunofluorescence and time lapse cinematography, endosomes containing FSH were observed to be translocated to perinuclear regions by a saltatory movement followed by streaming. The streaming was attended by reorganization of both MT and IF. In addition, drug treatments that disrupted MT and IF were shown to block the translocation of endosomes.

We have been unable to produce direct evidence that the structural associations repeatedly observed between cytoskeletal elements and subcellular organelles containing Au_{16}-hCG were actually functionally related to the internalization process. However, the structural relationships between cytoskeletal elements and compartments involved in endocytosis of Au_{16}-hCG were strikingly similar to those described in granulosa cells (4,3,14,64,65), and probably do contribute functionally to the internalization process, by mechanisms that remain to be determined.

H. Conclusions

We developed and characterized a new probe, Au_{16}-hCG, and have used this probe to monitor the endocytosis of hormone by fully differentiated porcine luteal cells. Au_{16}-hCG appeared to be internalized by luteal cells along a traditional receptor-mediated pathway. Following internalization, Au_{16}-hCG was transferred to initial endosomes that resembled morphologically the receptosome of the fibroblast, and the body of CURL in the hepatocyte. Au_{16}-hCG subsequently appeared in Golgi-associated regions and lysosome like structures. Cytoskeletal elements were abundant along the endocytic pathway, and were repeatedly observed to establish direct structural interactions with membranes of subcellular organelles labeled with Au_{16}-hCG. Whether these structural interactions are important to the successful completion of RME remains to be determined.

LIST OF REFERENCES

LIST OF REFERENCES

1. Abel, J.H., T.T. Chen, D.B. Endres, M.C. McClellen, M.A. Diekman, H.R. Sawyer, G.D. Niswender, M.H.J. Schmitz and M.P. Pineda. 1978. "Sites of Binding and Metabolism of Gonadotropic Hormones in the Mammalian Ovary." In: Cell Membrane Receptors for Drugs and Hormones: A Multidisciplinary Approach. Straus and Bolis, New York. pp. 183-201.

2. Ackerman, G.A. and K.W. Wolken. 1980. Differential Surface Labeling, Uptake, and Subcellular Translocation of Colloidal Gold Labeled Insulin Complex by Normal Blood Cells. IRCS Med Sci-Biochem 8:842-843.

3. Albertini, D.F. and E. Anderson. 1977. Microtubule and Microfilament Rearrangements during Capping of Concanavalin A Receptors on Cultured Ovarian Granulosa Cells. J. Cell Biol. 73:111-127.

4. Albertini, D.F. and J.I. Clark. 1975. Membrane-Microtubule Interactions: Concanavalin A Capping Induced Redistribution of Cytoplasmic Microtubules and Colchicine Binding Proteins. Proc. Natl. Acad. Sci. USA 12:4976-4980.

5. Amsterdam, A., A. Berkowitz, A. Nimrod and K. Fortuna. 1980. Aggregation of Luteinizing Hormone Receptors in Granulosa Cells: A Possible Mechanism of Desensitization to the Hormone. Proc. Natl. Acad. Sci. USA 6:3440-3444.

6. Amsterdam, A., A. Nimrod, S.A. Lamprecht, Y. Burstein and H.R. Lindner. 1979. Internalization and Degradation of Receptor Bound hCG in Granulosa Cell Cultures. Am. J. Physiol. 236:E129-E138.

7. Anderson, R.G.W., M.S. Brown, V. Bersiegel and J.L. Goldstein. 1982. Surface Distribution and Recycling of the Low Density Lipoprotein Receptor as Visualized with Antireceptor Antibodies. J. Cell Biol. 93:523-531.

8. Anderson, R.G.W., M.S. Brown and J.L. Goldstein. 1977. Role of the Coated Endocytic Vesicle in the Uptake of Receptor-bound Low Density Lipoprotein in Human Fibroblasts. Cell 10:351-364.

9. Anderson, R.G.W., J.L. Goldstein and M.S. Brown. 1976. Localization of Low Density Lipoprotein Receptors on Plasma Membrane of Normal Human Fibroblasts and their Absence in Cells from a Familial Hypercholesterolemia Homozygote. Proc. Natl. Acad. Sci. USA 75:2434-2438.

10. Anderson, W., Y-H. King, M.E. Perotti, T.A. Brandeis and R.J. Ryan. 1979. Interactions of Gonadotropins with Corpora Luteum Membranes. III. Electron Microscopic Localization of ^{125}I-hCG Binding to Sensitive and Desensitized Ovaries Seven Days after PMSG-hCG. Biol. Reprod. 20:362-376.

11. Ash, J.F., D. Louvard and S.J. Singer. 1977. Antibody Induced Linkages of Plasma Membrane Proteins to Intracellular Actomyosin Containing Filaments in Cultured Fibroblasts. Proc. Natl. Acad Sci. USA 74:5584-5588.

12. Ash, J.F. and S.J. Singer. 1976. Concanavalin A-induced Transmembrane Linkage of Concanavalin A Surface Receptors to Intracellular Myosin Containing Filaments. Proc. Natl. Acad. Sci. USA 73:4575-4579.

13. Basu, S.K., J.C. Goldstein, R.G.W. Anderson and M.S. Brown. 1981. Monensin Interrupts the Recycling of Low Density Lipoprotein Receptors in Human Fibroblasts. Cell 24:493-502.

14. Batten, B.E., J.J. Aalberg and E. Anderson. 1980. The Cytoplasmic Filamentous Network in Cultured Ovarian Granulosa Cells. Cell 21:885-895.

15. Begg, D.A., R. Rodewald and L.L. Rebhun. 1978. The Visualization of Actin Filament Polarity in Thin Sections. J. Cell Biol. 79:846-852.

16. Bergeron, J.M., B.I. Posner, Z. Josefsberg and R. Sirstrom. 1978. Intracellular Polypeptide Hormone Receptors: The Demonstration of Specific Binding Sites for Insulin and Human Growth Hormone in Golgi Fractions Isolated from the Liver of Female Rats. J. Cell Biol. 253:4058-4066.

17. Bloch, R.J. and Z.W. Hall. 1983. Cytoskeletal Components of the Vertebrate Neuromuscular Junction: Vinculin, α-Actinin and Filamen. J. Cell Biol. 97:217-223.

18. Bowen-Pope, D.F., P.E. Dicorleto and R. Ross. 1983. Interactions Between the Receptors for Platelet-derived Growth Factor and Epidermal Growth Factor. J. Cell Biol. 96:679-683.

19. Bradford, M. 1976. A Rapid and Sensitive Method for the Quantitation of Microgram Quantities of Protein Utilizing the Principle of Protein-dye Binding. Analytical Biochem. 72:248-254.

20. Branton, D., C.M. Cohen and J. Tyler. 1981. Interaction of Cytoskeletal Proteins on the Human Erythrocyte Membrane. Cell 24:24-32.

21. Bridges, K., J. Harford, G. Ashinell and R.D. Kansoner. 1982. Fate of Receptor and Ligand during Endocytosis of Asialoglycoproteins by Isolated Hepatocytes. Proc. Natl. Acad. Sci. USA 79:350-354.

22. Brown, M.S. and J.L. Goldstein. 1979. Receptor-mediated Endocytosis: Insights from the Lipoprotein Receptor System. Proc. Natl. Acad. Sci. USA 76:3330-3337.

23. Carpentier, G. and S. Cohen. 1976. ^{125}I-labeled Human Epidermal Growth Factor. Binding, Internalization, and Degradation in Human Fibroblasts. J. Cell Biol. 71:159-171.

24. Carpentier, J.L., P. Gorden, M. Amherdt, E. Van Obberghen, C.R. Kaha and L. Orci. 1978. ^{125}I-Insulin Binding to Cultured Human Lymphocytes: Initial Localization and Fate of Hormone Determined by Quantitative Electron Microscopic Autoradiography. J. Canc. Invest. 61:1056-1070.

25. Carpentier, J.L., P. Gorden, P. Freychet and A. LeCam. 1979. Lysosomal Association of Internalized ^{125}I-Insulin in Isolated Rat Hepatocytes: Direct Demonstration by Quantitative Electron Microscopic Autoradiography. J. Clin. Invest. 63:1249-1261.

26. Carpentier, J.L., P. Gorden, J.L. Goldstein, R.G.W. Anderson, M.S. Brown and L. Orci. 1979. Binding and Internalization of ^{125}I-LDL in Normal and Mutant Human Fibroblasts. Exp. Cell Res. 121:135-142.

27. Carpentier, J.L., E.V. Obberglen, P. Gorden and L. Orci. 1981. Binding, Membrane Redistribution, Internalization, and Lysosomal Association of ^{125}I-Anti-Insulin Receptor Antibody in IM-9 Cultured Human Lymphocyte. Exp. Cell Res. 134:81-92.

28. Carsten, M. and E. Mommaerts. 1963. A Study of Actin by Means of Starch Gel Electrophoresis. Biochem. 1:28-32.

29. Channing, C.P. and S. Kammerman. 1974. Binding of Gonadotropins to Ovarian Cells. Biol. of Reprod. 10:179-198.

30. Chen, T.T., J.H. Abel, M.C. McClellan, H.R. Sawyer, M.A. Diekman and G.D. Niswender. 1977. Localization of Gonadotropic Hormones in Lysosomes of Ovine Luteal Cells. Cytobiologie 14:412-420.

31. Chen, T.T., M.C. McClellan, M.A. Diekman, J.H. Abel and G.D. Niswender. 1978. Localization of Human Chorionic Gonadotropin in Lysosomes of Ovine Luteal Cells. Structure and Function of the Gonadotropins, Biochemical Endocrinology. Plenum Press, N.Y., pp. 591-612.

32. Cheng, S.Y., F.R. Maxfield, J. Robbins, M.C. Willingham and I. Pastan. 1980. Receptor-mediated Uptake of 3,3',5-triiodo-L-thyronine by Cultured Fibroblasts. Proc. Natl. Acad. Sci. USA 77:3425-3429.

33. Ciechanover, A., A.L. Schwartz and H. Lodish. 1983. The Asialoglycoprotein Receptor Internalizes and Recycles Independently of the Transferrin and Insulin Receptors. Cell 32:367-375.

34. Cohen, C.N., J.M. Tyler and D. Branton. 1980. Spectrin-Actin Associations Studied by Electron Microscopy of Shadowed Preparations. Cell 21:875-883.

35. Condeelis, J. 1979. Isolation of Concanavalin A Caps During Various Stages of Formation and their Association with Actin and Myosin. J. Cell Biol. 80:751-758.

36. Conn, M.P., C. Marco, J.P. Harwood, M.L. Dufau and K.J. Catt. 1978. Internalization of Gonadotrophin-Receptor Complex in Ovarian Luteal Cells. Nature 274:598-600.

37. Connally, D.T., R.R. Townsend, K. Kawaguchi, W.R. Bell and Y.C. Lee. 1982. Binding and Endocytosis of Cluster Glycosides by Rabbit Hepatocytes. Evidence for a Short Circuit Pathway that does not lead to Degradation. J. Biol. Chem. 257:939-945.

38. Conti, M., J.P. Harwood, M.L. Dufau and K.J. Catt. 1977. Effect of Gonadotropin-induced Receptor Regulation on Biological Responses of Isolated Rat Luteal Cells. J. Biol. Chem. 252:24:8869-8879.

39. Detmers, P., A. Weber, M. Elzinga and R.E. Stephens. 1981. 7-chloro-4-monobenzeno-2-oxa-1,3-diazole Actin as a Probe for Actin Polymerization. J. Biol. Chem. 256:10:99-105.

40. Dickson, R.B., R. Schlegel, M.C. Willingham and I.H. Pastan. 1982. Reversible and Irreversible Inhibitors of Clustering of α_2M in Clathrin Coated Pits on the Surface of Fibroblasts. Exp. Cell Res. 140:215-225.

41. Dickson, R.B., M.C. Willingham and I. Pastan. 1981. α_2Macroglobulin Adsorbed to Colloidal Gold. A New Probe in the Study of Receptor-mediated Endocytosis. J. Cell Biol. 89:29-34.

42. Farquhar, M.G. 1978. Recovery of Surface Membrane in Anterior Pituitary Cells. Variations in Traffic Detected with Anionic and Cationic Ferritin. J. Cell Biol. 77:R35-R42.

43. Farquhar, M.G. 1981. Membrane Recycling in Secretory Cells: Implications for Traffic of Products and Specialized Membranes within the Golgi Complex. In: Methods in Cell Biology, Vol. 23, Academic Press, New York, pp. 400-427.

44. Fitz, T.A., H.R. Sawyer and G.D. Niswender. 1981. Characterization of Two Steroidogenic Cell Types in the Ovine Corpus Luteum. Biol. Reprod. SI. 24:54A.

45. Fitzgerald, D., R.E. Morris and C.B. Saelinger. 1980. Receptor-mediated Internalization of Pseudomonas Toxin by Mouse Fibroblasts. Cell 21:867-873.

46. Fitzgerald, D., R. Padmanbhan, I. Pastan and M.C. Willingham. 1983. Adenorious-induced Release of Epidermal Growth Factor and Pseudomonas Toxin into the Cytosol of KB Cells during Receptor-mediated Endocytosis. Cell 32:607-617.

47. Freeman, D.E. and M. Ascoti. 1981. Desensitization to Gonadotropins in Cultured Leydig Tumor Cells Involves Loss of Gonadotropin Receptors and Decreased Capacity for Steroidogenesis. Proc. Natl. Acad. Sci. USA 78:10:63-9-6313.

48. Geoghegan, W.D. and G.A. Ackerman. 1977. Adsorption of Horseradish Peroxidase, Ovomucoid and Anti-immunoglobulin to a Colloidal Gold for the Indirect Detection of Concanavalin A, Wheat Germ Agglutinin, and Goat Anti-human Immunoglobulin. J. Histochem. Cytochem. 25:1187-1200.

49. Geuze, H.J., J.W. Slot, J.A.M. Strous, H. Lodish and A.L. Schwartz. 1983. Intracellular Site of Asiaglycoprotein Receptor-Ligand Uncoupling: Double-Label Immunoelectron Microscopy during Receptor-Mediated Endocytosis. Cell 32:277-287.

50. Goldman, R.D., B. Chojnacki and M.-J. Yerva. 1979. Ultrastructure of Microfilament Bundles in Baby Hamster Kidney (BHK-21) Cells. The Use of Tannic Acid. J. Cell Biol. 80:759-766.

51. Goldstein, J.L., R.G.W. Anderson and M.S. Brown. 1979. Coated Pits, Coated Vesicles, and Receptor-Mediated Endocytosis. Nature 279:679-685.

52. Goldstein, J.L., S.K. Basu, G.Y. Brunschede and M.S. Brown. 1976. Release of Low Density Lipoprotein from its Cell Surface Receptor by Sulfated Glycosaminoglycans. Cell 7:85-95.

53. Gonatas, N.K., S.U. Kim, A. Stieber and S. Auraneas. 1977. Internalization of Lectins in Neuronal GERL. J. Cell Biol. 73:1-13.

54. Gonatas, J., A. Stiebers, S. Olsnes and N.K. Gonatas. 1970. Pathways Involved in Fluid Phase and Absorptive Pinocytosis in Neuroblastoma. J. Cell Biol. 87:754-765.

55. Gonzalez-Noriega, A., J.H. Grubb, V. Talkad and W.S. Sly. 1980. Chloroquine Inhibits Lysosomal Enzyme Photocytosis and Enhances Lysosomal Enzyme Secretion by Impairing Receptor Recycling. J. Cell Biol. 85:839-852.

56. Gorden, P., J.L. Carpentier, J-Y. Fan and L. Orci. 1982. Receptor-Mediated Endocytosis of Polypeptide Hormones: Mechanisms and Significance. Metabolism 31:664-669.

57. Gospodarowicz, D. 1973. Properties of the Luteinizing Hormone Receptor of Isolated Bovine Corpus Luteum Plasma Membranes. J. Biol. Chem. 248:14:5042-5049.

58. Green, A. and I.M. Olefsky. 1982. Evidence for Insulin-induced Internalization and Degradation of Insulin Receptors in Rat Adipocytes. Proc. Natl. Acad. Sci. USA 79:427-431.

59. Haigler, H.T., F.R. Maxfield, M.C. Willingham and I. Pastan. 1980. Dansylcadaverine Inhibits Internalization of ^{125}I-Epidermal Growth Factor in BALB-3T3 Cells. J. Biol. Chem. 255:4:1239-1241.

60. Haigler, H.T., J.A. McKanna and S. Cohen. 1979. Direct Visualization of the Binding and Internalization of a Ferritin Conjugate of Epidermal Growth Factor in Human Carcinoma Cells A-431. J. Cell Biol. 81:382-395.

61. Handley, D.A., C.M. Arbeeny, L.D. Witte and S. Chien. 1981. Colloidal-Gold Low Density Lipoprotein Conjugates as Membrane Receptor Probes. Proc. Natl. Acad. Sci. USA 78:1:368-371.

62. Harwood, J.P., M. Conti, P.M. Conn, M.L. Dufau and K.J. Catt. 1978. Receptor Regulation and Target Cell Responses: Studies in the Ovarian Luteal Cell. Biol. and Cell Endocrinol. 11:121-135.

63. Helenius, A., J. Kartenbede, K. Simms and E. Fries. 1980. On the Entry of Semliki Forrest Virus into BHK-21 cells. J. Cell Biol. 84:404-420.

64. Herman, B. and D.F. Albertini. Role of the Cytoskeleton During Endosome Translocations in Ovarian Granulosa Cells. J. Cell Biol. 95:440a.

65. Herman, B. and D.F. Albertini. Time Lapse Video Image Intensification Analysis of Endosome and Lysosome Movements in Cultured Granulosa Cells. J. Cell Biol. 95:440a.

66. Herzog, V. 1980. Pathways of Endocytosis from Luminal Plasma Membrane in Rat Exocrine Pancreas. Eur. J. Biochem. 21:141-150.

67. Herzog, V. 1981. Pathways of Endocytosis in Secretory Cells. Trends in Biomed. Sci. 6:12:319-322.

68. Herzog, V. and M.G. Farquhar. 1977. Luminal Membrane Retrieval After Exocytosis Reaches Most Golgi Cisternae in Secretory Cells. Proc. Natl. Acad. Sci. USA 74:11:5073-5077.

69. Higuchi, T., A. Kaneko, J.H. Abel and G.D. Niswender. 1976. Relationship Between Membrane Potential and Progesterone Release in Ovine Corpora Lutea. Endo. 99:4:1023-1032.

70. Hirokawa, N., L.G. Tilney, K. Fujiwara and J.E. Heuser. 1982. Organization of Actin, Myosin, and Intermediate Filaments in the Brush Border of Intestinal Epithelial Cells. J. Cell Biol. 94:425-443.

71. Hizuka, N., P. Gorden, M.A. Lesniak, E. Van Obberghen, J-L. Carpentier and L. Orci. 1981. Polypeptide Hormone Degradation and Receptor Regulation are Coupled to Ligand Internalization. J. Biol. Chem. 256:9:4591-4597.

72. Hollenberg, M.D. 1979. Hormone Receptor Interactions at the Cell Membrane. Pharmacological Reviews 30:4:393-410.

73. Horisberger, M. 1979. Evaluation of Colloidal Gold as a Cytochemical Marker for Transmission and Scanning Electron Microscopy. Biologie Cellulaire 36:3:253-261.

74. Horisberger, M. 1981. Colloidal Gold: A Cytochemical Marker for Light and Fluorescent Microscopy and for Transmission and Scanning Electron Microscopy. In: Scanning Electron Microscopy. A. M. F. O'Hare, Chicago. pp. 9-31.

75. Horisberger, M. and J. Rosset. 1977. Colloidal Gold, a Useful Marker for Transmission and Scanning Electron Microscopy. J. Histochem. Cytochem. 25:4:295-305.

76. Huxley, H.E. 1963. Electron Microscope Studies on the Structure of Natural and Synthetic Protein Filaments from Striated Muscle. J. Molec. Biol. 7:281-308.

77. Ishikawa, H., R. Bischoff and H. Holtzer. 1969. Formation of Arrowhead Complexes with Heavy Meromyosin in a Variety of Cell Types. J. Cell Biol. 43:312-328.

78. Johnson, K.A. and E.W. Taylor. 1978. Intermediate States of Subfragments-1 and Actosubfragments-1 ATPase: Re-evaluation of the Mechanism. Biochem. 417:3432-3442.

79. Kammerman, S., Canfield, R.E., J. Kolena and C.P. Channing. 1972. The Binding of Iodinated hCG to Porcine Granulosa Cells. Endocrinol. 91:1:65-74.

80. Kaplan, J. 1980. Evidence of Reutilization of Surface Receptors for α_2M Protease Complexes in Rabbit Alveolar Macrophages. Cell 19:197-205.

81. Karin, M. and B. Mintz. 1981. Receptor-Mediated Endocytosis of Transferrin in Developmentally Totipotent Mouse Tetracarcinoma Stem Cells. J. Biol. Chem. 256:3245-3252.

82. Lemon, M. and M. Loir. 1977. Steroid Release in Vitro by Two Luteal Cell Types in the Corpus Luteum of the Pregnant Sow. J. Endocrinol. 72:351-359.

83. Lemon, M. and P. Mauleon. 1982. Interaction Between Two Luteal Cell Types from the Corpus Luteum of the Sow in Progesterone Synthesis in Vitro. J. Reprod. Fert. 64:315-323.

84. Levine, J. and M. Willard. 1981. Fodrin: Axonally Transported Polypeptides Associated with the Internal Perifery of Many Cells. J. Cell Biol. 90:631-643.

85. Lovell, S.J., P.J. Knight and W.F. Harrington. 1981. Fraction of Myosin Heads Bound to Thin Filaments in Rigor Fibrils from Insect Flight and Vertebrate Muscles. Nature 293:5834:664-666.

86. Lowey, S., H.S. Slayter, A.G. Weeds and H. Baker. 1969. Substructure of the Myosin Molecule. I. Subfragments of the Myosin by Enzymic Degradation. J. Mol. Biol. 42:1-29.

87. Luborsky, J.L. and H.R. Behrman. 1979. Localization of LH Receptors on Luteal Cells with a Ferritin-LH Conjugate. Molecular and Cellular Endocrinol. 15:61-78.

88. Luna, E.J., V.M. Fowler, J. Swanson, D. Branton and D.L. Taylor. 1981. A Membrane Cytoskeleton from Dictyostelium Discoideum. I. Identification and Partial Characterization of an Actin-Binding Activity. J. Cell Biol. 88:396-409.

89. Marsh, M. and A. Helenius. 1980. Absorptive Endocytosis of Semliki Forest Virus. J. Molec. Biol. 142:439-454.

90. Marshall, S., A. Green and J. Olefsky. 1981. Evidence for the Recycling of Insulin Receptors in Isolated Rat Adipocytes. J. Biol. Chem. 256:11464-11470.

91. Maxfield, F.R., J. Schlessinger, Y. Schechter, I. Pastan and M.C. Willingham. 1978. Collection of Insulin, EGF, and α_2Macroglobulin in the same Patches on the Surface of Cultured Fibroblasts and Common Internalization. Cell 14:805-810.

92. Maxfield, F.R., M.C. Willingham, H.T. Haigler, P. Dragsten and I.H. Pastan. 1981. Binding, Surface Mobility, Internalization, and Degradation of Rhodamine-labeled α_2-Macroglobulin. Biochem. 20:5353-5358.

93. Maxfield, F.R., M.C. Willingham, I. Pastan, P. Dragsten and S.Y. Cheng. 1981. Binding and Mobility of the Cell Surface Receptors for 3,3,5-triiodo-L-Thyronine. Science 211:63-65.

94. Moore, P.B., H.E. Huxley and D.J. DeRosier. 1970. Three-Dimensional Reconstruction of F-Actin, Thin Filaments, and Decorated Thin Filaments. J. Molec. Biol. 50:279-295.

95. Mooseker, M.S. and L.G. Tilney. 1975. Organization of an Actin Filament-Membrane Complex: Filament Polarity and Membrane Attachment in the Microvilli of Intestinal Epithelial Cells. J. Cell Biol. 67:725-743.

96. Muller, W.A., R.M. Steinman and A.A. Cohn. 1982. The Membrane Proteins of the Vacuolar System. III. Further Studies on the Composition and Recycling of Endocytic Vacuole Membrane in Cultured Macrophages. J. Cell Biol. 96:29-36.

97. Novikoff, A.B. 1976. The Endoplasmic Reticulum: A Cytochemist's View. Proc. Natl. Acad. Sci. USA 78:8:2781-2787.

98. Novikoff, A.B. and P.M. Novikoff. 1977. Cytochemical Contributions to Differentiating GERL from the Golgi Apparatus. Histochem. J. 9:525-551.

99. Oliver, C. and A.R. Hand. 1981. Membrane Retrieval in Exocrine Acinar Cells. In: Methods in Cell Biology, Vol. 23. Academic Press, NY. pp. 429-444.

100. Orci, L. 1981. Exocytosis-Endocytosis. In: Methods in Cell Biology, Vol. 23, Academic Press, NY. pp. 283-300.

101. Ottosen, P.D., P.J. Courtoy and M.G. Farquhar. 1980. Pathways Followed by Membrane Recovered from the Surface of Plasma Cells and Myeloma Cells. J. Exp. Med. 152:1-9.

102. Pastan, I.H. and M.C. Willingham. 1981. Journey to the Center of the Cell: Role of the Receptosome. Science 214:504-509.

103. Pastan, I.H. and M.C. Willingham. 1981. Receptor-Mediated Endocytosis of Hormones in Cultured Cells. Ann. Rev. Phys. 43:239-250.

104. Peterson, O.W. and B. Van Deurs. 1983. Serial-Section Analysis of Coated Pits and Vesicles Involved in Adsorptive Pinocytosis in Cultured Fibroblasts. J. Cell Biol. 96:277-281.

105. Phillips, D.R. and M. Morrison. 1971. Exposed Protein on the Intact Human Erythrocyte. Biochem. 10:1766-1771.

106. Phillips, H.J. 1973. Dye Exclusion Tests for Cell Viability. In Tissue Culture: Methods and Applications, Academic Press NY, 406-408.

107. Philipson, L., K. Lonberg-Holon and V. Pettersson. 1968. Virus-Receptor Interaction in an Adenovirus System. J. Virol. 2:1064-1075.

108. Pilch, P.F., M.A. Shia, R.J. Benson and R.E. Fine. 1983. Coated Vesicles Participate in the RME of Insulin. J. Cell Biol. 93:133-138.

109. Rao, C.U. 1975. Mechanism of Nucleotide Inhibition of Gonadotropin Binding to Cell Membranes of Bovine Corpus Luteum. Molec. Cell Endo. 3:255-271.

110. Rao, C.V., S. Mitra and F.R. Carmen. 1981. Characterization of Gonadotropin Binding Sites in the Intracellular Organelles of Bovine Corpora Lutea and Comparison with Plasma Membrane Sites. J. Biol. Chem. 256:6:2628-2634.

111. Rao, C.V. and B.B. Saxena. 1973. Gonadotropin Receptors in the Plasma Membranes of Rat Luteal Cells. Biochem. Biophys. Acta 313:372-389.

112. Rodewald, R. 1980. Distribution of Immunoglobulin G Receptors in the Small Intestine of the Young Rat. J. Cell Biol. 85:18-32.

113. Salisbury, J.L., J.S. Condeelis and P. Satir. 1980. Role of Coated Vesicles, Microfilaments, and Calmodulin in Receptor-Mediated Endocytosis by Cultured β-Lymphoblastoid Cells. J. Cell Biol. 87:132-141.

114. Sawyer, H.R., J.H. Abel, M.C. McClellan, M. Schmitz and G.D. Niswender. 1979. Secretory Granules and Progesterone Secretion by Ovine Corpora Lutea in Vitro. Endocrinol. 104:2:476-486.

115. Schlessinger, J., Y. Schnechter, M.C. Willingham and I. Pastan. 1978. Visualization of Binding, Aggregation, and Internalization of Insulin, and Epidermal Growth Factor on Living Fibroblastic Cells. Proc. Natl. Acad. Sci. USA 75:6:2659-2663.

116. Schloss, J.A., A. Milsted and R.D. Goldman. 1977. Myosin Subfragment Binding for the Localization of Actin-like Microfilaments in Cultured Cells. J. Cell Biol. 74:794-815.

117. Schmitz, M.H.J., J.H. Abel, T.T. Chen, M.C. McClellan, H.R. Sawyer and G.D. Niswender. 1978. The Role of Calcium in Progesterone Synthesis and Release in Ovarian Granulosa Lutein Cells. J. Cell Biol. 79:371a.

118. Silverstein, S.C., R.M. Steinman and Z.A. Cohn. 1977. Endocytosis. Ann. Rev. Biochem. 46:669-722.

119. Simmons, K.R., J.L. Caffney, J.L. Phillips, J.H. Abel and G.D. Niswender. 1976. A Simple Method for Preparing Suspensions of Luteal Cells. Soc. Exp. Biol. Med. 152:366-371.

120. Spudich, J.A. and S. Watt. 1971. The Regulation of Rabbit Skeletal Muscle Contraction. J. Biol. Chem. 246:15:4866-4871.

121. Stahl, P., P.H. Schlessinger, E. Sigardson, J.J. Rodman and Y.C. Lee. 1980. Receptor-mediated Pinocytosis of Mannose Glycoconjugated by Macrophages: Characterization and Evidence for Receptor Recycling. Cell 19:207-215.

122. Stair, R. and G. Offer. 1971. Polypeptide Chains of Intermediate Molecular Weight in Myosin Preparations. F.E.B.S. Letters 15:1:40-44.

123. Steinman, R.M., I.S. Mellman, W.A. Muller and Z.A. Cohn. 1983. Endocytosis and the Recycling of Plasma Membrane. J. Cell Biol. 96:1-27.

124. Steinman, R.M., J.M. Silver and Z.A. Cohn. 1974. Pinocytosis in Fibroblasts: Quantitative Studies in Vitro. J. Cell Biol. 63:949-969.

125. Szentgyorgy, E.M. 1961. The Binding of H-Meromyosin on Cross-Striated Myofibrils. Exp. Cell Res. 22:18-30.

126. Tietze, C., P. Schlessinger and P. Stahl. 1982. Mannose-Specific Endocytosis Receptor of Alveolar Macrophages: Demonstration of Two Functionally Distinct Intracellular Pools of Receptor and Their Roles in Receptor Recycling. J. Cell Biol. 92:417-424.

127. Tilney, L.G., E.H. Egelman, D.J. DeRosier and J.C. Saunders. 1983. Actin Filaments, Stereocilia, and Hair Cells of the Bird Cochlea. II. Packing of Actin Filaments in the Stereocilia and in the Cuticular Plate, and What Happens to the Organization When the Stereocilia are Bent. J. Cell Biol. 96:822-834.

128. Tilney, L.G. and J.C. Saunders. 1983. Actin Filaments, Stereocilia, and Hair Cells of the Bird Cochlea. I. Length, Numbers, Width, and Distribution of Stereocilia of Each Hair Cell are Related to the Position of the Hair Cell on the Cochlea. J. Cell Biol. 96:807-821.

129. Tyko, B. and F.R. Maxfield. 1982. Rapid Acidification of Endocytic Vesicles Containing α_2-Macroglobulin. Cell 28:643-651.

130. Wall, D.A., G. Wilson and A.L. Hubbard. 1980. The Galactose-Specific Recognition System of Mammalian Liver: The Route of Ligand Internalization in Rat Hepatocytes. Cell 21:79-93.

131. Weatherbee, J.A. 1981. Membranes and Cell Movement: Interactions of Membranes with the Proteins of the Cytoskeleton. International Rev. Cytol. Suppl. 12, Academic Press, NY. pp. 113-175.

132. Weber, K. and A. Osborn. 1969. The Reliability of Molecular Weight Determination by Dodecyl Sulfate-Polyacrylamide Gel Electrophoresis. J. Biol. Chem. 244:4406-4412.

133. Weeds, A. 1982. Actin-Binding Proteins: Regulators of Cell Architecture and Motility. Nature 296:811-816.

134. Weeds, A.G. and B. Pope. 1977. Studies on the Chymotrypitic Digestion of Myosin: Effects of Divalent Cations on Proteolytic Suseptibility. J. Molec. Biol. 111:129-157.

135. Weeds, A.G. and R.S. Taylor. 1975. Separation of Subfragment-1: Isoenzymes from Rabbit Skeletal Muscle Myosin. Nature 257:54-56.

136. White, J., K. Matlin and A. Helenius. 1981. Cell Fusion by Semliki Forest Influenza, and Vesicular Stomatilis Viruses. J. Cell Biol. 89:674-679.

137. Wiley, H.S. and D.D. Cunningham. 1982. The Endocytic Rate Constant. J. Biol. Chem. 257:8:4222-4229.

138. Willingham, M.C. and I. Pastan. 1980. The Receptosome: An Intermediate Organelle of Receptor-Mediated Endocytosis in Cultured Fibroblasts. Cell 21:67-77.

139. Willingham, M.C., I.H. Pastan and G.G. Sakagian. 1983. Ultrastructural Immunocytochemical Localization of the Phosphomannosyl Receptor in Chinese Hamster Ovary (CHO) Cells. J. Histochem. Cytochem. 31:1:1-11.

140. Willingham, M.C., S.S. Yamada and I. Pastan. 1978. Ultrastructural Localization of Alpha-2-Macroglobulin in Membrane-Limited Vesicles in Cultured Cells. Proc. Natl. Acad. Sci. 75:4359-4363.

141. Zigmond, S.H., S.J. Sullivan, D.A. Lauffenburger. 1982. Kinetic Analysis of Chemotactic Peptide Receptor Modulation. J. Cell Biol. 92:34-43.

142. Zimniski, S.J., E.A. Rorke, S. Helmy and J.L. Vaitukaitus. 1982. Characterization of Human Chorionic Gonadotropin Internalized by Pseudopregnant Rat Ovary. Endocrinol. 111:2:635-640.

143. Zimniski, S.J., E.A. Rorke, M.A. Sickel and J.L. Vaitukaitus. 1982. Fate of Human Chorionic Gonadotropin Bound to Rat Corpora Lutea. Endocrinol. 111:2:625-634.

VITA

Lisa Leigh Satterwhite was born on November 19, 1956 in Asheville, N.C. She attended Sand Hill Elementary School in Asheville, and graduated from Enka High School, Enka, N.C. in June, 1975. The following September she enrolled at The University of Tennessee at Knoxville. In 1980 she received a Bachelor of Arts degree from the College of Liberal Arts with a double major in Medical Illustration and Art History. In September, 1980 she began graduate studies in the Department of Zoology at UTK with Dr. John H. Abel as her major advisor. Ms. Satterwhite completed the Master of Science degree, in March, 1984. During the last year of graduate study, she was also employed as Research Assistant to Dr. N.B. Gilula at Baylor College of Medicine in Houston, Texas.